PHYSICAL REVIEW D **88,** 125021 (2013)

Quark sector of the QCD groundstate in Coulomb gauge

M. Pak[1,*] and H. Reinhardt[2,†]

[1]*Institut für Physik, FB Theoretische Physik, Universität Graz, Universitätsplatz 5, 8010 Graz, Austria*
[2]*Institut für Theoretische Physik, Universität Tübingen, Auf der Morgenstelle 14, 72076 Tübingen, Germany*
(Received 7 October 2013; published 10 December 2013)

The variational approach to Yang-Mills theory in Coulomb gauge is extended to full QCD. For the quark sector we use a trial wave functional, which goes beyond the previously used BCS-type state and which explicitly contains the coupling of the quarks to transverse gluons. This quark wave functional contains two variational kernels: one is related to the quark condensate and occurs already in the BCS-type states; the other represents the form factor of the coupling of the quarks to the transverse gluons. Minimization of the energy density with respect to these kernels results in two coupled integral (gap) equations. These equations are solved numerically using the confining part of the non-Abelian color Coulomb potential and the lattice static gluon propagator as input. With the additional coupling of quarks to transverse gluons included, the low energy chiral properties increase substantially towards their phenomenological values. We obtain a reasonable description of the chiral condensate, which for a vanishing current quark mass is obtained in the range of 190–235 MeV. The coupling of the quarks to the transverse gluons enhances the constituent quark mass by about 60% in comparison to the pure BCS *Ansatz*.

DOI: 10.1103/PhysRevD.88.125021 PACS numbers: 11.30.Rd, 12.38.Aw

I. INTRODUCTION

Understanding the low energy sector of QCD is one of the major challenges of particle physics. This sector is characterized by two nonperturbative phenomena: confinement and chiral symmetry breaking. Color confinement is assumed to be essentially due to the gluon sector. In recent years, substantial progress in understanding the low energy sector of Yang-Mills theory has been achieved within nonperturbative continuum approaches. Among these is a variational approach to Yang-Mills theory in Coulomb gauge, Ref. [1]. There is a long history of the variational treatment of the Yang-Mills vacuum sector in Coulomb gauge; see, for example, Refs. [2,3]. Our approach differs from previous work in the choice of the trial wave functional and, more importantly, in the full inclusion of the Faddeev-Popov determinant and in the renormalization procedure; see Ref. [4] for more details. Our variational approach has given a quite decent description of the infrared sector of Yang-Mills theory as, for example, a linearly rising non-Abelian Coulomb potential [5], an infrared diverging gluon energy (expressing confinement) [1,5] in accord with lattice data [6], an infrared finite running coupling constant [7], a perimeter law for the 't Hooft loop [8], an area law for the Wilson loop [9], and a dielectric function of the Yang-Mills vacuum in accord with the bag model picture [10]. The obtained infrared behaviors of ghost and gluon propagators were also found in a functional renormalization group approach [11] and supported by lattice calculation [6,12]. Furthermore, recently the variational approach of Ref. [1] was extended to finite temperatures [13,14]. A critical temperature in the range of $T_C = 270$–290 MeV was obtained [14], which is in the range of the lattice data [15–17]. A similar transition temperature of $T_C \approx 270$ MeV was also found from the effective potential of the Polyakov loop [18,19].

In the present paper we extend the variational approach in Coulomb gauge to full QCD. The low energy quark sector of QCD is dominated by chiral symmetry and its spontaneous breaking. For N_f massless quark flavors QCD is invariant under separate global flavor rotations of the left- and right-handed quarks. In the vacuum, the $U_L(N_f) \times U_R(N_f)$ symmetry group is spontaneously broken to the diagonal vector group $U_V(N_f)$ by quark condensation $\langle \bar{q}q \rangle \neq 0$, resulting in the appearance of N_f^2 pseudoscalar massless Goldstone bosons corresponding to the generators of the coset $U_A(N_f) = U_L(N_f) \times U_R(N_f)/U_V(N_f)$. Chiral symmetry is a good starting point for $N_f = 3$ quark flavors u, d, s. When the small current quark masses of the light flavors are included, chiral symmetry is explicitly broken and the (would-be) Goldstone bosons acquire a finite mass. Finally, the chiral anomaly breaks the $U_A(N_f)$ down to $SU_A(N_f)$, thereby providing an extra mass to the Goldstone boson of the $U_A(1)$ generator, which corresponds to the η' meson.

The mechanism of spontaneous breaking of chiral symmetry was first investigated in effective models of the Nambu–Jona-Lasinio type, Refs. [20,21], which could explain the quark condensation in analogy to the emergence of Cooper pairs in superconductors. The Nambu–Jona-Lasinio model has been successful not only in explaining the mechanism of spontaneous breaking of chiral symmetry but also in describing the low energy data of the light pseudoscalar mesons. For this purpose, the

*markus.pak@uni-graz.at
†hugo.reinhardt@uni-tuebingen.de

Nambu–Jona-Lasinio model was bosonized and the resulting effective meson theory was worked out in a gradient expansion [22]. Inspired by these model studies, the quark sector of QCD was treated in the variational approach in Coulomb gauge, assuming BCS-type trial quark wave functionals and a purely confining static quark potential, Refs. [23–25]. Equivalent to the use of the BCS-type trial wave function is to carry out a Bogoliubov-Valatin transformation (see also Ref. [26]). In these calculations, the coupling of the transverse gluons to the quarks was neglected, resulting in substantially too small values of the quark condensate, the constituent mass, and pion decay constant. To improve these results in Refs. [27,28], an additional four-quark interaction mediated by static transverse gluons was introduced; see also Ref. [29]. Of course, an additional attractive interaction will enhance the amount of chiral symmetry breaking. However, such a four-fermion interaction mediated by transverse gluons is not in the QCD Hamiltonian in Coulomb gauge in the first place. Neither does this Hamiltonian contain an explicit coupling of the quarks to the transverse gluons and it is *a priori* not clear to which extent this coupling can be simulated by a static four-quark interaction. The quark-gluon coupling of the QCD Hamiltonian escapes the variational approach when a BCS-type trial wave functional is used. In the present paper, we go beyond the BCS type of approximations considered previously and use a quark wave functional, which explicitly includes the coupling to the transverse gluons. The form factor of this coupling is treated as a variational kernel determined from the minimization of the energy. First results obtained with this wave functional have been already reported in Ref. [30]. Here we give a more detailed and complete account of the variational approach to QCD in Coulomb gauge with the trial wave functional proposed in Ref. [30].

We will find that the coupling of the quarks to the transversal gluon field substantially increases the amount of chiral symmetry breaking. At the same time, we show that when neglecting the four-quark interaction of the gauge-fixed QCD Hamiltonian, the coupling of the quarks to the transversal gluons alone does not trigger spontaneous breaking of chiral symmetry.

Though the variational approach can, in principle, be carried out in a fully self-consistent manner, minimizing simultaneously the energy with respect to all kernels of the trial wave functional, in order to keep the formal exposition sufficiently transparent in the present paper, we will focus on the quark sector and do mainly a quenched calculation, ignoring the backreaction of the quarks on the gluon sector; i.e., we will use the results obtained in the variational approach to Yang-Mills theory, in particular the gluon dispersion relation, as an input. However, in Sec. XI we will study the effect of the quarks on the gluon propagator.

Let us also mention that an alternative approach to including the quark-gluon coupling along with the confining non-Abelian Coulomb interaction is to use Dyson-Schwinger equations in Coulomb gauge [31–33].

The organization of the paper is as follows: in Sec. II we review the Hamiltonian approach to QCD in Coulomb gauge. In Sec. III we briefly collect results gained in the pure Yang-Mills sector of QCD, which are needed as input for the present work. In Sec. IV we present our quark vacuum wave functional, which includes the interaction of quarks with transverse gluon fields and which was originally proposed in Ref. [30]. The Dirac and color structure of the variational kernels are specified. In Sec. V we set up the QCD generating functional in order to compute the various n-point functions of the theory. In Sec. VI the quark propagator and related chiral quantities are expressed in terms of the variational functions. In Sec. VII we start our variational analysis by computing the energy density of the quarks and carry out the variation of the latter with respect to the two kernels of the wave functional, resulting in two coupled gap equations. These equations are studied in Sec. VIII in the IR and UV regime. In a first variational analysis, we demonstrate in Sec. IX that within the present approach, the coupling of the quarks to the transverse gluons alone cannot induce spontaneous breaking of chiral symmetry. The full variational calculation with the color Coulomb potential included is carried out in Sec. X. Here we solve the corresponding coupled gap equation numerically and calculate the chiral properties of the quarks. In Sec. XI we give an estimate of the unquenching effects on the gluon propagator. In the last section, Sec. XII, we summarize our findings, present our conclusions, and give an outlook on future studies.

II. HAMILTONIAN APPROACH TO QCD IN COULOMB GAUGE

The Hamiltonian approach to QCD is based on the canonical quantization in Weyl gauge $A_0 = 0$, which leaves the spatial components of the gauge field $\boldsymbol{A}(\boldsymbol{x})$ as independent coordinates and results in the Hamiltonian

$$H_{\text{QCD}} = H_{\text{YM}} + H_{\text{F}}, \tag{1}$$

where

$$H_{\text{YM}} = \frac{1}{2}\int d^3x (\boldsymbol{\Pi}^2(\boldsymbol{x}) + \boldsymbol{B}^2(\boldsymbol{x})) \tag{2}$$

is the Yang-Mills Hamiltonian, with

$$B_k^a(\boldsymbol{x}) = \varepsilon_{klm}(\nabla_l A_m^a(\boldsymbol{x}) + f^{abc} A_l^b(\boldsymbol{x}) A_m^c(\boldsymbol{x}))$$

being the non-Abelian magnetic field (f^{abc}-structure constant of the gauge group) and

$$\boldsymbol{\Pi}^a(\boldsymbol{x}) = \frac{\delta}{i\delta \boldsymbol{A}^a(\boldsymbol{x})} \tag{3}$$

being the conjugate momentum operator. Furthermore,

$$H_{\mathrm{F}} = \int d^3x \psi^\dagger(\boldsymbol{x})(-i\boldsymbol{\alpha}\cdot\boldsymbol{D} + \beta m_0)\psi(\boldsymbol{x}) \tag{4}$$

is the Hamilton operator of the quark field $\psi(\boldsymbol{x})$, which satisfies the anticommutation relation

$$\{\psi(\boldsymbol{x}), \psi^\dagger(\boldsymbol{y})\} = \delta(\boldsymbol{x}-\boldsymbol{y}). \tag{5}$$

Here $\boldsymbol{\alpha}$, β are the usual Dirac matrices satisfying $\{\alpha_i, \alpha_j\} = \delta_{ij}$ and $\{\beta, \alpha_i\} = 0$, m_0 is the current quark mass, and

$$\boldsymbol{D} = \boldsymbol{\partial} - igT^a\boldsymbol{A}^a \tag{6}$$

is the covariant derivative with T^a being the (Hermitian) generators of the gauge group $SU(N)$ in the fundamental representation. We have suppressed here the Lorentz, color, and flavor indices of the quarks. For the present consideration, it is sufficient to consider a single flavor so that flavor becomes irrelevant. Due to the use of Weyl gauge, Gauss's law escapes the equation of motion and has to be imposed as a constraint to the wave functional $\phi[\boldsymbol{A}, \psi]$

$$(\hat{\boldsymbol{D}}^{ab}\boldsymbol{\Pi}^b)(\boldsymbol{x})\phi[\boldsymbol{A}, \psi] = \rho_{\mathrm{F}}^a(\boldsymbol{x})\phi[\boldsymbol{A}, \psi]. \tag{7}$$

Here

$$\hat{\boldsymbol{D}}^{ab} = \delta^{ab} + gf^{acb}\boldsymbol{A}^c \tag{8}$$

is the covariant derivative in the adjoint representation, and

$$\rho_{\mathrm{F}}^a(\boldsymbol{x}) = \psi^\dagger(\boldsymbol{x})T^a\psi(\boldsymbol{x}) \tag{9}$$

are the color charge densities of the quarks. The operator $\hat{\boldsymbol{D}}^{ab}\boldsymbol{\Pi}^b$ in Gauss's law is the generator of time-independent gauge transformations, which are not fixed by Weyl gauge. We fix this residual gauge freedom by choosing the Coulomb gauge

$$\boldsymbol{\partial}\boldsymbol{A} = 0. \tag{10}$$

In this gauge Gauss's law can be explicitly resolved, which results in the gauge-fixed Hamiltonian [34]

$$\bar{H}_{\mathrm{QCD}} = \bar{H}_{\mathrm{YM}} + \bar{H}_F + \bar{H}_C, \tag{11}$$

where $\bar{H}_{\mathrm{F}}$ is the same as H_F in (4) except that the gauge field is now transversal:

$$A_i^{\perp a}(\boldsymbol{x}) = t_{ij}(\boldsymbol{x})A_j^a(\boldsymbol{x}), \tag{12}$$

with

$$t_{ij}(\boldsymbol{x}) = \int \frac{d^3p}{(2\pi)^3}(\delta_{ij} - \hat{p}_i\hat{p}_j)e^{i\boldsymbol{p}\cdot\boldsymbol{x}}, \qquad \hat{p}_i = \frac{p_i}{|\boldsymbol{p}|}. \tag{13}$$

Furthermore,

$$\bar{H}_{\mathrm{YM}} = \frac{1}{2}\int d^3x(J^{-1}[\boldsymbol{A}^\perp]\Pi_i^{\perp a}(\boldsymbol{x})J[\boldsymbol{A}^\perp]\Pi_i^{\perp a}(\boldsymbol{x}) + B_i^a(\boldsymbol{x})^2) \tag{14}$$

is the Hamiltonian of the transverse gluons, where

$$\Pi_i^{\perp a}(\boldsymbol{x}) = \frac{\delta}{i\delta A_i^{\perp a}(\boldsymbol{x})} = t_{ij}(\boldsymbol{x})\Pi_j^a(\boldsymbol{x}), \tag{15}$$

and

$$J[\boldsymbol{A}^\perp] = \mathrm{Det}(-\hat{\boldsymbol{D}}\boldsymbol{\partial}) \tag{16}$$

is the Faddeev-Popov determinant. The Coulomb term

$$\bar{H}_{\mathrm{C}} = \frac{g^2}{2}\int d^3x\int d^3y J^{-1}[\boldsymbol{A}^\perp]\rho^a(\boldsymbol{x})F^{ab}(\boldsymbol{x},\boldsymbol{y}) \times J[\boldsymbol{A}^\perp]\rho^b(\boldsymbol{y}) \tag{17}$$

arises from the kinetic energy of the longitudinal modes after resolving Gauss's law. Here

$$F^{ab}(\boldsymbol{x},\boldsymbol{y}) = \langle \boldsymbol{x}a|(-\hat{\boldsymbol{D}}\boldsymbol{\partial})^{-1}(-\boldsymbol{\partial}^2)(-\hat{\boldsymbol{D}}\boldsymbol{\partial})^{-1}|\boldsymbol{y}b\rangle \tag{18}$$

is the so-called Coulomb kernel and

$$\rho^a(\boldsymbol{x}) = \rho_{\mathrm{YM}}^a(\boldsymbol{x}) + \rho_{\mathrm{F}}^a(\boldsymbol{x}) \tag{19}$$

is the total color charge density, which contains besides the charge of the quarks, $\rho_{\mathrm{F}}^a(\boldsymbol{x})$ [Eq. (9)], also the color charge of the gauge field

$$\rho_{\mathrm{YM}}^a(\boldsymbol{x}) = -f^{abc}\boldsymbol{A}^{\perp b}(\boldsymbol{x})\boldsymbol{\Pi}^{\perp c}(\boldsymbol{x}). \tag{20}$$

In the rest of the paper, we work exclusively in Coulomb gauge and from now on we will omit the transversality sign attached to the gauge field.

We are interested here in the groundstate wave functional of QCD, which we approximate from a variational calculation. Without loss of generality, we can choose the trial wave functional in the coordinate representation of the gauge field in the form

$$|\phi(A)\rangle = \phi_{\mathrm{YM}}(\boldsymbol{A})|\phi_{\mathrm{F}}(\boldsymbol{A})\rangle. \tag{21}$$

Here $|\phi_{\mathrm{F}}(\boldsymbol{A})\rangle$ is the wave functional of the Dirac vacuum of the quarks in the presence of the gauge field and $\phi_{\mathrm{YM}}(\boldsymbol{A}) = \langle\boldsymbol{A}|\phi_{\mathrm{YM}}\rangle$ is the wave functional of the Yang-Mills sector. We have chosen here the coordinate representation for the Yang-Mills part of the wave functional $\phi_{\mathrm{YM}}(\boldsymbol{A})$, while the fermion wave functional $|\phi_{\mathrm{F}}(\boldsymbol{A})\rangle$ is chosen as ket vector in Fock space. Note $|\phi_{\mathrm{F}}(\boldsymbol{A})\rangle$, depending on the gauge field, contains the full coupling of the quarks to gluons.

The expectation value of an observable $O[\boldsymbol{A}, \psi]$ in the state (21) is given by

$$\langle O[\boldsymbol{A}, \psi]\rangle = \int \mathcal{D}\boldsymbol{A} J(A)\phi_{\mathrm{YM}}^*(\boldsymbol{A}) \times \langle\phi_F(\boldsymbol{A})|O[\boldsymbol{A}, \psi]|\phi_{\mathrm{F}}(\boldsymbol{A})\rangle\phi_{\mathrm{YM}}(\boldsymbol{A}). \tag{22}$$

Note the presence of the Faddeev-Popov determinant $J[A]$ [Eq. (16)] in the integration measure. In principle, the fermion wave functional $|\phi_F(\boldsymbol{A})\rangle$ could also be expressed in a "coordinate" representation, i.e., in terms of

Grassmann variables. Then the scalar product (22) would also contain the integration over Grassmann fields. In the present case it is, however, more convenient to represent the fermionic wave functional in second quantized form as a vector in Fock space; see Sec. IV.

With the color charge density $\rho^a(\boldsymbol{x})$ [Eq. (19)] being a sum of a gluonic and a quark part, the Coulomb Hamiltonian $\bar{H}_C$ [Eq. (17)] can be split up as

$$\bar{H}_C = \bar{H}_C^{YM} + \bar{H}_C^{coupl} + \bar{H}_C^F, \tag{23}$$

where $\bar{H}_C^{YM}$ and $\bar{H}_C^F$ depend exclusively on the charges of the gauge field $\boldsymbol{A}$ and the quark field ψ, respectively, while H_C^{coupl} contains the coupling between both charges. With this splitting we can write the full gauge-fixed QCD Hamiltonian (11) in the form

$$\bar{H}_{QCD} = \tilde{H}_{YM}(\boldsymbol{A}) + \tilde{H}_F(\boldsymbol{A}, \psi), \tag{24}$$

where

$$\tilde{H}_{YM}(A) = \bar{H}_{YM} + \bar{H}_C^{YM} \tag{25}$$

contains exclusively the gauge field and is the Coulomb gauge-fixed Hamiltonian of pure Yang-Mills theory (which was treated variationally in Ref. [1]), while

$$\tilde{H}_F(A, \psi) = \bar{H}_F + \bar{H}_C^F + \bar{H}_C^{coupl} \tag{26}$$

contains all terms which depend on the quark field. In particular, it contains the coupling of the quarks to the gluons; see Eq. (4).

In a full variational calculation one would minimize the full energy

$$\langle \bar{H}_{QCD} \rangle \rightarrow \min \tag{27}$$

in the state (21). Here we work in a quenched calculation, varying the fermionic part of the energy only,

$$\langle \tilde{H}_F \rangle \rightarrow \min, \tag{28}$$

thereby keeping the Yang-Mills part $\phi_{YM}(\boldsymbol{A})$ of the wave functional (21) fixed to the Yang-Mills vacuum state determined previously in Ref. [5] from

$$\langle \phi_{YM} | \tilde{H}_{YM} | \phi_{YM} \rangle \rightarrow \min. \tag{29}$$

In the next section, we will briefly summarize the essential results obtained within the variational approach to Yang-Mills theory (29), which we use as input for the variational treatment of the fermionic sector, Eq. (28).

III. VARIATIONAL RESULTS FOR THE PURE YANG-MILLS SECTOR OF QCD

In Refs. [1,5], pure Yang-Mills theory has been treated in a variational approach in Coulomb gauge using the following trial *Ansatz* for the vacuum wave functional:

$$\begin{aligned}\phi_{YM}(\boldsymbol{A}) &= \langle \boldsymbol{A} | \phi_{YM} \rangle \\ &= \frac{\mathcal{N}_G}{\sqrt{\mathcal{J}[\boldsymbol{A}]}} \exp\Big(-\frac{1}{2}\int d^3x \int d^3y A_i^a(\boldsymbol{x}) t_{ij}(\boldsymbol{x}) \\ &\quad \times \omega(\boldsymbol{x}, \boldsymbol{y}) A_j^a(\boldsymbol{y})\Big).\end{aligned} \tag{30}$$

Here $\mathcal{J}[\boldsymbol{A}]$ is the Faddeev-Popov determinant [Eq. (16)], $\mathcal{N}_G$ is a normalization factor fixed by requiring $\langle \phi_{YM} | \phi_{YM} \rangle = 1$, and $\omega(\boldsymbol{x}, \boldsymbol{y})$ is the variational kernel. The advantage of this *Ansatz* is that the Faddeev-Popov determinant $J[\boldsymbol{A}]$ [Eq. (16)] drops out from the integration measure (22). As a consequence, the (static or equal time) gluon propagator is just given by the inverse of the kernel ω:

$$\begin{aligned}&D_{ij}^{ab}(\boldsymbol{x}, \boldsymbol{y}) := \langle A_i^a(\boldsymbol{x}) A_j^b(\boldsymbol{y}) \rangle_G = \delta^{ab} t_{ij}(\boldsymbol{x}) D(\boldsymbol{x} - \boldsymbol{y}), \\ &D(\boldsymbol{x} - \boldsymbol{y}) = \frac{1}{2}\omega^{-1}(\boldsymbol{x}, \boldsymbol{y}),\end{aligned} \tag{31}$$

where

$$\langle \ldots \rangle_G = \langle \phi_{YM} | \ldots | \phi_{YM} \rangle \tag{32}$$

denotes the expectation value in the pure Yang-Mills vacuum state $|\phi_{YM}\rangle$ [Eq. (30)].

Variation of the pure gluonic energy density $\langle \bar{H}_{YM}^C \rangle_G$ [Eq. (25)] with respect to the kernel ω yields a coupled system of integral equations; see, e.g., Refs. [1,5]. These equations were solved analytically in the IR and UV asymptotic momentum regions (Ref. [7]), as well as numerically in the whole momentum regime (Refs. [1,5]). The gluon energy $\omega(\boldsymbol{p})$ is found to be IR divergent, expressing gluon confinement, while it approaches for large momenta the photon energy, in accord with asymptotic freedom. Lattice calculations (Ref. [6]) confirm this behavior and show that over the whole momentum range, the gluon kernel $\omega(\boldsymbol{p})$ can be nicely fitted by Gribov's formula [35]

$$\omega(\boldsymbol{p}) = \sqrt{\boldsymbol{p}^2 + \frac{M_G^4}{\boldsymbol{p}^2}}, \tag{33}$$

where M_G is a mass scale referred to as the Gribov mass. It was determined on the lattice in Ref. [6] and found to be given by

$$M_G \approx 880 \text{ MeV} = 2\sqrt{\sigma_W}, \tag{34}$$

where σ_W ($\sqrt{\sigma_W} = 440$ MeV) is the Wilsonian string tension. Figure 1 shows the gluon propagator obtained in the variational approach together with lattice data. The results obtained with the Gaussian wave functional (30) agree well with the lattice results in the IR and also in the UV, but there are deviations in the mid-momentum regime. These deviations substantially decrease when a non-Gaussian wave functional is used, which includes up to quartic terms in the exponent; see Ref. [36].

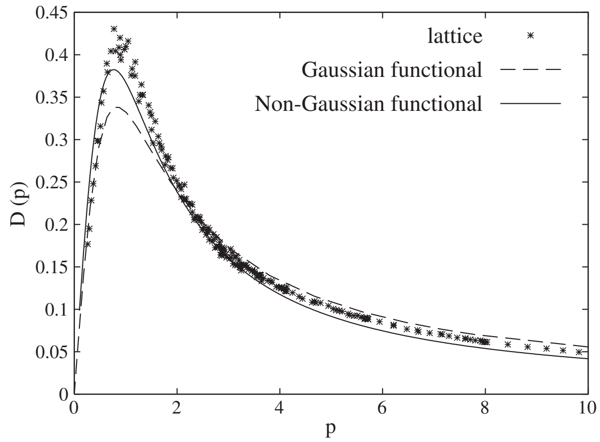

FIG. 1. Gluon propagator $D(p)$. Data points are the lattice results obtained in Ref. [6]. The dashed curve shows the results from the variational approach when a Gaussian vacuum is used. The full curve is the extension to non-Gaussian wave functionals including up to quartic terms in the gauge field. The plot is from Ref. [36].

In later calculations, we also need the vacuum expectation value of the Coulomb kernel $F(\boldsymbol{x}, \boldsymbol{y})$ [Eq. (18)], which represents the static potential between (infinitely heavy) color point charges separated by a distance $r = |\boldsymbol{x} - \boldsymbol{y}|$:

$$g^2 \langle F(\boldsymbol{x}, \boldsymbol{y}) \rangle_G := V_C(|\boldsymbol{x} - \boldsymbol{y}|). \tag{35}$$

In the variational approach [5], one finds a potential which at large distances increases linearly:

$$V_C(r) = \sigma_C r, \qquad r \to \infty. \tag{36}$$

The same behavior is found on the lattice, Refs. [37–39], with a Coulomb string tension σ_C of

$$\sigma_C \approx (2 \ldots 3)\sigma_W, \tag{37}$$

where σ_W is the Wilsonian string tension. In our approach, the Coulomb string tension σ_C is used to fix the scale. When we use the gluon propagator (33) as input there is a second dimensionful input quantity: the Gribov mass M_G. These two quantities are, however, not independent of each other. In the approximation

$$\begin{aligned} &\langle (-\hat{\boldsymbol{D}}\boldsymbol{\partial})^{-1}(-\boldsymbol{\partial}^2)(-\hat{\boldsymbol{D}}\boldsymbol{\partial})^{-1} \rangle_G \\ &\quad \simeq \langle (-\hat{\boldsymbol{D}}\boldsymbol{\partial})^{-1} \rangle_G (-\boldsymbol{\partial}^2) \langle (-\hat{\boldsymbol{D}}\boldsymbol{\partial})^{-1} \rangle_G \end{aligned} \tag{38}$$

to the Coulomb potential [Eqs. (35) and (18)], one finds from the IR analysis of the equations of motion of the pure Yang-Mills sector (see, e.g., Ref. [14]) the following relation:

$$\sigma_C = \frac{\pi}{N_C} M^2. \tag{39}$$

For $N_C = 3$ we can put $\pi/N_C \simeq 1$ and obtain the approximate relation

$$\sigma_C \simeq M_G^2. \tag{40}$$

With the lattice result $M_G \simeq 2\sqrt{\sigma_W}$, this yields $\sigma_C \simeq 4\sigma_W$, which shows that σ_C is larger than σ_W, in agreement with Ref. [40].

IV. THE QUARK VACUUM WAVE FUNCTIONAL

In this section we define our trial state for the quark vacuum $|\phi_F(\boldsymbol{A})\rangle$. For this purpose we decompose the fermion field $\psi(\boldsymbol{x})$ into positive and negative energy components

$$\psi(\boldsymbol{x}) = \psi_+(\boldsymbol{x}) + \psi_-(\boldsymbol{x}), \tag{41}$$

given by

$$\psi_\pm(\boldsymbol{x}) = \int d^3y \Lambda_\pm(\boldsymbol{x}, \boldsymbol{y}) \psi(\boldsymbol{y}), \tag{42}$$

$$\psi_\pm^\dagger(\boldsymbol{x}) = \int d^3y \psi^\dagger(\boldsymbol{y}) \Lambda_\pm(\boldsymbol{y}, \boldsymbol{x}), \tag{43}$$

where

$$\Lambda_\pm(\boldsymbol{x}, \boldsymbol{y}) = \int \frac{d^3p}{(2\pi)^3} e^{i\boldsymbol{p}\cdot(\boldsymbol{x}-\boldsymbol{y})} \Lambda_\pm(\boldsymbol{p}), \tag{44}$$

with

$$\Lambda_\pm(\boldsymbol{p}) = \frac{1}{2}\left(\mathbb{1} \pm \frac{h(\boldsymbol{p})}{E(\boldsymbol{p})}\right), \tag{45}$$

are the projectors onto positive (negative) energy eigenstates. Here $h(\boldsymbol{p})$ is the free Dirac Hamiltonian in momentum space

$$h(\boldsymbol{p}) = \boldsymbol{\alpha}\boldsymbol{p} + \beta m_0, \tag{46}$$

whose eigenvalues are $\pm E(\boldsymbol{p})$ with $E(\boldsymbol{p}) = \sqrt{\boldsymbol{p}^2 + m_0^2}$. The orthogonal projectors fulfill the relations

$$\Lambda_\pm^2 = \Lambda_\pm, \qquad \Lambda_\pm \Lambda_\mp = 0, \qquad \Lambda_\pm + \Lambda_\mp = \mathbb{1}. \tag{47}$$

From the anticommutation relation, Eq. (5), the nonvanishing anticommutation relations for the positive (negative) energy spinors follow:

$$\{\psi_\pm(\boldsymbol{x}), \psi_\pm^\dagger(\boldsymbol{y})\} = \Lambda_\pm(\boldsymbol{x}, \boldsymbol{y}), \quad \{\psi_\pm(x), \psi_\mp^\dagger(y)\} = 0. \tag{48}$$

The free (bare) fermion vacuum $|0\rangle$ is defined by

$$\psi_+(\boldsymbol{x})|0\rangle = 0, \qquad \psi_-^\dagger(\boldsymbol{x})|0\rangle = 0. \tag{49}$$

We choose our trial state $|\phi_F\rangle$ of the quark vacuum as the most general Slater determinant which is not orthogonal to the bare vacuum $|0\rangle$. By the Thouless theorem,[1] such a state has the form

[1] For a detailed proof, see Ref. [41].

$$|\phi_F\rangle = \mathcal{N}_F \exp\left[-\int d^3x \int d^3y \psi_+^\dagger(\boldsymbol{x}) K(\boldsymbol{x},\boldsymbol{y}) \psi_-(\boldsymbol{y})\right]|0\rangle, \tag{50}$$

where $\mathcal{N}_F$ is a normalization constant to be determined later. The use of a Slater determinant has the advantage that Wick's theorem applies, which facilitates the evaluation of expectation values of products of fermion operators. Since the wave functional (50) has to embody the coupling of the quarks to the gluons, the kernel $K(\boldsymbol{x},\boldsymbol{y})$ can in principle be any functional of the gauge field. We will assume here that $K(\boldsymbol{x},\boldsymbol{y})$ can be Taylor expanded in powers of the gauge field and that this expansion can be truncated in leading order:

$$K(\boldsymbol{x},\boldsymbol{y}) = K_0(\boldsymbol{x},\boldsymbol{y}) + \int d^3z \boldsymbol{K}(\boldsymbol{x},\boldsymbol{y};\boldsymbol{z})\boldsymbol{A}(\boldsymbol{z}) \equiv K_0(\boldsymbol{x},\boldsymbol{y}) + K_1(\boldsymbol{x},\boldsymbol{y}). \tag{51}$$

From the definition of the wave functional (50) and the projection properties (47), it follows that the variational kernel can be chosen to satisfy

$$\int d^3z \int d^3z' \Lambda_+(\boldsymbol{x},\boldsymbol{z}) K^{ij}(\boldsymbol{z},\boldsymbol{z}')\Lambda_-(\boldsymbol{z}',\boldsymbol{y}) = K^{ij}(\boldsymbol{x},\boldsymbol{y}). \tag{52}$$

Incorporating this property, we choose the variational kernels in the form

$$K_0(\boldsymbol{x},\boldsymbol{y}) = \int d^3x' \int d^3y' \Lambda_+(\boldsymbol{x},\boldsymbol{x}')\beta S(\boldsymbol{x}'-\boldsymbol{y}')\Lambda_-(\boldsymbol{y}',\boldsymbol{y}) \tag{53}$$

$$\boldsymbol{K}^a(\boldsymbol{x},\boldsymbol{y};\boldsymbol{z}) = \int d^3x' \int d^3y' \Lambda_+(\boldsymbol{x},\boldsymbol{x}')\boldsymbol{\alpha} T^a \times V(\boldsymbol{x}'-\boldsymbol{y}', \boldsymbol{z}-\boldsymbol{y}')\Lambda_-(\boldsymbol{y}',\boldsymbol{y}), \tag{54}$$

where the form factors $S(\boldsymbol{x})$ and $V(\boldsymbol{x},\boldsymbol{y})$ are the variational functions to be determined by minimizing the energy density. The choice of the position arguments in the variational functions is dictated by translational invariance. Furthermore, the Lorentz and color structure of the variational kernel (54) is basically dictated by Lorentz and color symmetry since the vacuum wave function has to be a color and Lorentz scalar. Of course, more complicated (tensor structures and) *Ansätze* in the exponent are possible, but the present one can be considered as the leading nontrivial order of the expansion of the exponent of the wave functional in powers of the gauge field.

For $V(\boldsymbol{x},\boldsymbol{y}) = 0$, the wave functional $|\phi_F\rangle$ [Eq. (50)], with the kernel K [Eqs. (51), (53), and (54)], reduces to the BCS state considered in Refs. [23–25]. The new element is the vector coupling $\boldsymbol{K}(\boldsymbol{x},\boldsymbol{y}) \sim V(\boldsymbol{x},\boldsymbol{y})$ [Eq. (54)].

For the explicit calculation, it is convenient to express the variational kernel $K^{ab}(\boldsymbol{x},\boldsymbol{y})$ in Eq. (50) in momentum space ($\bar{d}^3p = \frac{d^3p}{(2\pi)^3}$):

$$K_0(\boldsymbol{x},\boldsymbol{y}) = \int \bar{d}^3p e^{i\boldsymbol{p}\cdot(\boldsymbol{x}-\boldsymbol{y})}\Lambda_+(\boldsymbol{p})\beta S(\boldsymbol{p})\Lambda_-(\boldsymbol{p}), \tag{55}$$

$$\boldsymbol{K}^a(\boldsymbol{x},\boldsymbol{y};\boldsymbol{z}) = \int \bar{d}^3p \bar{d}^3q e^{i\boldsymbol{p}\cdot(\boldsymbol{x}-\boldsymbol{y})}e^{i\boldsymbol{q}\cdot(\boldsymbol{z}-\boldsymbol{y})} \times \Lambda_+(\boldsymbol{p})\boldsymbol{\alpha}T^a V(\boldsymbol{p},\boldsymbol{p}+\boldsymbol{q})\Lambda_-(\boldsymbol{p}+\boldsymbol{q}). \tag{56}$$

The adjoint kernels read

$$K_0^\dagger(\boldsymbol{x},\boldsymbol{y}) = \int \bar{d}^3p e^{i\boldsymbol{p}\cdot(\boldsymbol{x}-\boldsymbol{y})}\Lambda_-(\boldsymbol{p})\beta S^*(\boldsymbol{p})\Lambda_+(\boldsymbol{p}), \tag{57}$$

$$\boldsymbol{K}^{\dagger a}(\boldsymbol{x},\boldsymbol{y};\boldsymbol{z}) = \int \bar{d}^3p \bar{d}^3q e^{i\boldsymbol{p}\cdot(\boldsymbol{x}-\boldsymbol{y})}e^{-i\boldsymbol{q}\cdot(\boldsymbol{z}-\boldsymbol{x})} \times \Lambda_-(\boldsymbol{p}+\boldsymbol{q})\boldsymbol{\alpha}T^a V^*(\boldsymbol{p}+\boldsymbol{q},\boldsymbol{p})\Lambda_+(\boldsymbol{p}), \tag{58}$$

where $*$ means complex conjugation. The scalar variational function $S(\boldsymbol{p})$ is dimensionless while the vector kernel $V(\boldsymbol{p},\boldsymbol{q})$ has dimension of inverse momentum.

V. THE QUARK GENERATING FUNCTIONAL

For the evaluation of the expectation values of quark observables, it is convenient to introduce the fermionic generating functional

$$Z_F[\eta] = \langle\phi_F|\exp\left[\int(\eta_+^*\psi_+ + \eta_-\psi_-^\dagger)\right] \times \exp\left[\int(\psi_+^\dagger\eta_+ + \psi_-\eta_-^*)\right]|\phi_F\rangle, \tag{59}$$

where $|\phi_F\rangle$ is the quark vacuum state (50) and η_+, η_- are the quark sources, which are Grassmann valued Dirac spinors. Since $|\phi_F\rangle$ is a Slater determinant, the generating functional can be evaluated in closed form. One finds after straightforward calculation

$$Z_F[\eta] = |\mathcal{N}_F|^2 \mathrm{Det}[\Omega]\exp[\eta^\dagger\Omega^{-1}\eta], \tag{60}$$

where we have introduced the bispinor notation

$$\eta = \begin{pmatrix} \eta_+ \\ -\eta_- \end{pmatrix}, \tag{61}$$

with the matrix Ω defined by

$$\Omega = \begin{pmatrix} 1 & K \\ K^\dagger & -1 \end{pmatrix}. \tag{62}$$

Here $\mathbb{1}$ denotes the unit kernel in the $\overset{+}{(-)}$ subspace of positive (negative) energy eigenstates. For vanishing source η, we find from Eq. (60)

$$Z_F[\eta = 0] \equiv \langle\phi_F|\phi_F\rangle = |\mathcal{N}_F|^2 \mathrm{Det}[\Omega]. \tag{63}$$

Note the norm of $|\phi_F\rangle$ is in principle a functional of the transverse gauge field $\boldsymbol{A}$ through the kernel K [Eq. (51)]. In a fully unquenched calculation, only the total QCD wave functional (21) can be normalized. However, in the quenched calculation, the Yang-Mills part and the fermionic part can be separately normalized. For a quenched calculation, we choose the normalization $\langle\phi_F|\phi_F\rangle = 1$, which removes the fermion determinant $\mathrm{Det}[\Omega]$ from the generating functional (60):

$$Z_F[\eta] = \exp[\eta^\dagger\Omega^{-1}\eta]. \tag{64}$$

This equation is a compact form of Wick's theorem and allows us to express all fermionic expectation values in terms of the matrix Ω^{-1}. Its gluonic expectation value $\langle\Omega^{-1}\rangle_G$ is closely related to the quark propagator; see Eq. (77) below.

The matrix Ω [Eq. (62)] can be explicitly inverted, yielding

$$\Omega^{-1} = \begin{pmatrix} [\mathbb{1} + KK^\dagger]^{-1} & [\mathbb{1} + KK^\dagger]^{-1}K \\ [\mathbb{1} + K^\dagger K]^{-1}K^\dagger & -[\mathbb{1} + K^\dagger K]^{-1} \end{pmatrix}. \tag{65}$$

Resolving the bispinor structure (61) the fermion generating functional (64) becomes

$$Z_F = \exp(\eta_+^*[\mathbb{1} + KK^\dagger]^{-1}\eta_+ - \eta_-^*[\mathbb{1} + K^\dagger K]^{-1}K^\dagger\eta_+ - \eta_+^*[\mathbb{1} + KK^\dagger]^{-1}K\eta_- - \eta_-^*[\mathbb{1} + K^\dagger K]^{-1}\eta_-). \tag{66}$$

Note that the matrix Ω [Eq. (62)], and hence also Ω^{-1} [Eq. (65)], is overall Hermitian.

With the explicit form of Ω^{-1} at hand from Eq. (64) or (66), all fermionic correlation functions can be evaluated. From the form of the generating functional (64), it follows that all fermionic correlation functions can be expressed in terms of the two-point functions, which is a manifestation of Wick's theorem. For later use we list the nonvanishing two-point functions

$$\langle\psi_+^i(\boldsymbol{x})\psi_+^{\dagger j}(\boldsymbol{y})\rangle_F = -\frac{\delta^2 Z[\eta]}{\delta\eta_+^{*i}(\boldsymbol{x})\delta\eta_+^j(\boldsymbol{y})}\bigg|_{\eta=0} = (\Lambda_+[\mathbb{1} + KK^\dagger]^{-1}\Lambda+)^{ij}(\boldsymbol{x},\boldsymbol{y}), \tag{67a}$$

$$\langle\psi_-^{\dagger i}(\boldsymbol{x})\psi_-^j(\boldsymbol{y})\rangle_F = -\frac{\delta^2 Z[\eta]}{\delta\eta_-^i(\boldsymbol{x})\delta\eta_-^{*j}(\boldsymbol{y})}\bigg|_{\eta=0} = (\Lambda_-[\mathbb{1} + K^\dagger K]^{-1}\Lambda_-)^{ji}(\boldsymbol{y},\boldsymbol{x}), \tag{67b}$$

$$\langle\psi_-^i(\boldsymbol{x})\psi_+^{\dagger j}(\boldsymbol{y})\rangle_F = \frac{\delta^2 Z[\eta]}{\delta\eta_-^{*i}(\boldsymbol{x})\delta\eta_+^j(\boldsymbol{y})}\bigg|_{\eta=0} = (\Lambda_-[\mathbb{1} + K^\dagger K]^{-1}K^\dagger\Lambda_+)^{ij}(\boldsymbol{x},\boldsymbol{y}), \tag{67c}$$

$$\langle\psi_+^i(\boldsymbol{x})\psi_-^{\dagger j}(\boldsymbol{y})\rangle_F = \frac{\delta^2 Z[\eta]}{\delta\eta_+^{*i}(\boldsymbol{x})\delta\eta_-^j(\boldsymbol{y})}\bigg|_{\eta=0} = (\Lambda_+[\mathbb{1} + KK^\dagger]^{-1}K\Lambda_-)^{ij}(\boldsymbol{x},\boldsymbol{y}), \tag{67d}$$

where the subscript F denotes the fermion expectation value in the state $|\phi_F\rangle$ [Eq. (50)]. Using the anticommutation relations (48), we obtain from Eqs. (67a) and (67b)

$$\langle\psi_+^{\dagger i}(\boldsymbol{x})\psi_+^j(\boldsymbol{y})\rangle_F = (\Lambda_+[\mathbb{1} + KK^\dagger]^{-1}KK^\dagger\Lambda_+)^{ji}(\boldsymbol{y},\boldsymbol{x}), \tag{68a}$$

$$\langle\psi_-^i(\boldsymbol{x})\psi_-^{\dagger j}(\boldsymbol{y})\rangle_F = (\Lambda_-[\mathbb{1} + K^\dagger K]^{-1}K^\dagger K\Lambda_-)^{ij}(\boldsymbol{x},\boldsymbol{y}). \tag{68b}$$

Through the kernel K, the fermionic expectation values $\langle\ldots\rangle_F$ are still functionals of the transverse gauge field. To find the true correlation functions, we still have to take the gluonic vacuum expectation value of the fermionic averages $\langle\ldots\rangle_F$. Fortunately, for the Yang-Mills wave functional (30), Wick's theorem applies. Nevertheless due to the presence of the inverse kernels $(1 + K^\dagger K)^{-1}$ in the fermionic correlation functions, the gluonic expectation values $\langle\ldots\rangle_G$ defined by Eq. (32) cannot be taken in closed form. To simplify the calculation, we will use the following approximation for inverse fermionic kernels:

$$\langle\cdots(\mathbb{1} + K^\dagger K)^{-1}\ldots\rangle_G \simeq \langle\ldots(\mathbb{1} + \langle K^\dagger K\rangle_G)^{-1}\ldots\rangle_G, \tag{69}$$

i.e., replacing in the inverse operators the kernels $K^\dagger K$ and $KK^\dagger$ by their expectation values $\langle K^\dagger K\rangle_G$ and $\langle KK^\dagger\rangle_G$, respectively. For the Yang-Mills wave functional (30), one finds with the explicit form of K [Eq. (51)]

$$\begin{aligned}\langle K^\dagger K\rangle_G &= K_0^\dagger K_0 + \langle K_1^\dagger K_1\rangle_G,\\ \langle KK^\dagger\rangle_G &= K_0 K_0^\dagger + \langle K_1 K_1^\dagger\rangle_G,\end{aligned} \tag{70}$$

with

$$\langle (K_1^\dagger K_1)_{mn}(\boldsymbol{x},\boldsymbol{y})\rangle_G = \int d^3z\int d^3z'(K_i^{\dagger a})_{ml}(\boldsymbol{x},\boldsymbol{x}';\boldsymbol{z})(K_j^b)_{ln} \times(\boldsymbol{x}',\boldsymbol{y};\boldsymbol{z}')D_{ij}^{ab}(\boldsymbol{z},\boldsymbol{z}'), \tag{71}$$

$$\langle (K_1 K_1^\dagger)_{mn}(\boldsymbol{x},\boldsymbol{y})\rangle_G = \int d^3z\int d^3z'(K_i^a)_{ml}(\boldsymbol{x},\boldsymbol{x}';\boldsymbol{z})(K_j^{\dagger b})_{ln} \times(\boldsymbol{x}',\boldsymbol{y};\boldsymbol{z}')D_{ij}^{ab}(\boldsymbol{z},\boldsymbol{z}'), \tag{72}$$

where $D_{ij}^{ab}(\boldsymbol{z},\boldsymbol{z}')$ is the gluon propagator (31). Here we have used that $\langle K_0^\dagger K_1\rangle_G = 0 = \langle K_1 K_0^\dagger\rangle_G$, since expectation values of an odd number of gluon fields vanish in the Gaussian vacuum, Eq. (30).

For the study of spontaneous breaking of chiral symmetry, the small current quark mass is irrelevant. Therefore from now on we will put $m_0 = 0$, which will simplify the explicit calculations and, in particular, the form of the projectors (44), which then satisfy the relation $\beta\Lambda_-(\boldsymbol{p}) = \Lambda_+(\boldsymbol{p})\beta$. With the explicit form of the kernels K_0 [Eq. (55)] and $\boldsymbol{K}$ [Eq. (56)], one finds after straightforward calculation

$$(K_0^\dagger K_0)(\boldsymbol{x}, \boldsymbol{y}) = \int đ^3 p e^{i\boldsymbol{p}\cdot(\boldsymbol{x}-\boldsymbol{y})} S^*(\boldsymbol{p}) S(\boldsymbol{p}) \Lambda_+(\boldsymbol{p}), \tag{73a}$$

$$(K_0 K_0^\dagger)(\boldsymbol{x}, \boldsymbol{y}) = \int đ^3 p e^{i\boldsymbol{p}\cdot(\boldsymbol{x}-\boldsymbol{y})} S(\boldsymbol{p}) S^*(\boldsymbol{p}) \Lambda_-(\boldsymbol{p}), \tag{73b}$$

$$\langle (K_1^\dagger K_1)_{mn}(\boldsymbol{x}, \boldsymbol{y}) \rangle_G = \delta_{mn} \int đ^3 p e^{i\boldsymbol{p}\cdot(\boldsymbol{x}-\boldsymbol{y})} R(\boldsymbol{p}) \Lambda_+(\boldsymbol{p}), \tag{73c}$$

$$\langle (K_1 K_1^\dagger)_{mn}(\boldsymbol{x}, \boldsymbol{y}) \rangle_G = \delta_{mn} \int đ^3 p e^{i\boldsymbol{p}\cdot(\boldsymbol{x}-\boldsymbol{y})} R(\boldsymbol{p}) \Lambda_-(\boldsymbol{p}). \tag{73d}$$

Here we have introduced the loop integral

$$R(\boldsymbol{p}) = C_F \int đ^3 q V(\boldsymbol{p}, \boldsymbol{q}) V^*(\boldsymbol{q}, \boldsymbol{p}) D(\boldsymbol{\ell}) \times [1 + (\hat{\boldsymbol{p}} \cdot \hat{\boldsymbol{\ell}})(\hat{\boldsymbol{q}} \cdot \hat{\boldsymbol{\ell}})], \tag{74}$$

where $\boldsymbol{\ell} = \boldsymbol{p} - \boldsymbol{q}$. Furthermore,

$$D(\boldsymbol{\ell}) = 1/(2\omega(\boldsymbol{\ell})) \tag{75}$$

is the Fourier transform of the spatial gluon propagator, Eq. (31), and $C_F = (N_C^2 - 1)/(2N_C)$ arises from the quadratic Casimir.

VI. THE QUARK PROPAGATOR

To investigate the properties of the quarks in the correlated QCD vacuum, the quantity of central interest is the (static or equal time) quark propagator

$$G_{rs}(\boldsymbol{x}, \boldsymbol{y}) = \langle \phi | \frac{1}{2} [\psi_r(\boldsymbol{x}), \psi_s^\dagger(\boldsymbol{y})] | \phi \rangle. \tag{76}$$

Working out the fermionic expectation value by means of the generating functional (59) and (64), one finds in the bispinor representation

$$G = \langle \Omega^{-1} \rangle_G - \frac{1}{2} \begin{pmatrix} 1 & 0 \\ 0 & -1 \end{pmatrix}. \tag{77}$$

To resolve the bispinor structure, it is more convenient to split the quark fields in Eq. (76) into their positive and negative energy components [see Eqs. (41)–(43)] and use Eqs. (67a)–(67d). This yields the alternative representation

$$\begin{aligned} G = \langle &\Lambda_+ (\mathbb{1} + KK^\dagger)^{-1} (\mathbb{1} - KK^\dagger) \Lambda_+ \\ &+ \Lambda_- (K^\dagger K - \mathbb{1})(\mathbb{1} + K^\dagger K)^{-1} \Lambda_- \\ &+ \Lambda_- (\mathbb{1} + K^\dagger K)^{-1} K^\dagger \Lambda_+ \\ &+ \Lambda_+ (\mathbb{1} + KK^\dagger)^{-1} K \Lambda_- \rangle_G. \end{aligned} \tag{78}$$

Taking now the expectation value in the gluonic Gaussian vacuum, Eq. (30), thereby using the approximation (69) and the explicit form of $\langle K^\dagger K \rangle_G, \langle KK^\dagger \rangle_G$ [Eq. (70)], we eventually obtain for the Fourier transform of the quark propagator

$$G(\boldsymbol{p}) = \frac{1}{2} \left[\frac{S(\boldsymbol{p}) + S^*(\boldsymbol{p})}{1 + S^*(\boldsymbol{p}) S(\boldsymbol{p}) + R(\boldsymbol{p})} \beta + \frac{1 - S^*(\boldsymbol{p}) S(\boldsymbol{p}) - R(\boldsymbol{p})}{1 + S^*(\boldsymbol{p}) S(\boldsymbol{p}) + R(\boldsymbol{p})} \boldsymbol{\alpha} \hat{\boldsymbol{p}} \right]. \tag{79}$$

It is interesting to note that the vectorial variational kernel $V(\boldsymbol{p}, \boldsymbol{q})$ enters the static quark propagator only via the loop integral $R(\boldsymbol{p})$ [Eq. (74)]. Setting the vector kernel $V(\boldsymbol{p}, \boldsymbol{q})$ to zero, this loop integral vanishes. Due to the approximation (69), the quantity $R(\boldsymbol{p})$ [Eq. (74)] contains the whole effect of the coupling of the quarks to the transverse spatial gluons.

The quark propagator (79) has the expected Dirac structure

$$G^{-1}(\boldsymbol{p}) = A(\boldsymbol{p}) \boldsymbol{\alpha} \boldsymbol{p} + B(\boldsymbol{p}) \beta = A(\boldsymbol{p})(\boldsymbol{\alpha} \boldsymbol{p} + \beta M(\boldsymbol{p})), \tag{80}$$

where

$$M(\boldsymbol{p}) = \frac{B(\boldsymbol{p})}{A(\boldsymbol{p})} \tag{81}$$

is the effective quark mass. Inversion of Eq. (80) yields

$$G(\boldsymbol{p}) = \frac{\boldsymbol{\alpha} \cdot \boldsymbol{p} A(\boldsymbol{p}) + \beta B(\boldsymbol{p})}{\boldsymbol{p}^2 A^2(\boldsymbol{p}) + B^2(\boldsymbol{p})}. \tag{82}$$

Comparing this representation with the explicit form (79) we obtain the following identifications:

$$\frac{1}{2} \frac{S(\boldsymbol{p}) + S^*(\boldsymbol{p})}{1 + S^*(\boldsymbol{p}) S(\boldsymbol{p}) + R(\boldsymbol{p})} = \frac{B(\boldsymbol{p})}{B^2(\boldsymbol{p}) + \boldsymbol{p}^2 A^2(\boldsymbol{p})}, \tag{83}$$

$$\frac{1}{2} \frac{1 - S^*(\boldsymbol{p}) S(\boldsymbol{p}) - R(\boldsymbol{p})}{1 + S^*(\boldsymbol{p}) S(\boldsymbol{p}) + R(\boldsymbol{p})} = \frac{A(\boldsymbol{p}) |\boldsymbol{p}|}{B^2(\boldsymbol{p}) + \boldsymbol{p}^2 A^2(\boldsymbol{p})}. \tag{84}$$

Dividing Eq. (83) by Eq. (84), we find for the effective quark mass (81)

$$M(\boldsymbol{p}) = |\boldsymbol{p}| \frac{S(\boldsymbol{p}) + S^*(\boldsymbol{p})}{1 - S^*(\boldsymbol{p}) S(\boldsymbol{p}) - R(\boldsymbol{p})}. \tag{85}$$

For a nonvanishing scalar form factor $S(\boldsymbol{p})$ [i.e., for nonvanishing quark-antiquark correlations, see Eqs. (50), (51), and (54)], a quark mass is dynamically generated. This dynamical mass generation is a consequence of the spontaneous breaking of chiral symmetry, which is signaled by a nonvanishing quark condensate:

$$\langle\bar{\psi}^i(\boldsymbol{x})\psi^i(\boldsymbol{x})\rangle = -\int đ^3p\,\mathrm{tr}[\beta G(\boldsymbol{p})]. \tag{86}$$

Inserting here the explicit form of the quark propagator (79), we find

$$\langle\bar{\psi}^i(\boldsymbol{x})\psi^i(\boldsymbol{x})\rangle = -N_C 2\int đ^3p\frac{S(\boldsymbol{p})+S^*(\boldsymbol{p})}{1+S^*(\boldsymbol{p})S(\boldsymbol{p})+R(\boldsymbol{p})}. \tag{87}$$

Obviously, a nonvanishing quark condensate requires $S(\boldsymbol{p})\neq 0$. Thus, a wave functional (50) with vector coupling only $[S(\boldsymbol{p})=0]$ cannot yield spontaneous breaking of chiral symmetry. Whether chiral symmetry is spontaneously broken is a dynamical question and requires the determination of the kernels $S(\boldsymbol{p})$ and $V(\boldsymbol{p},\boldsymbol{q})$ in the quark wave functional (50). This will be done in the following sections by means of the variational approach.

VII. ENERGY DENSITIES AND GAP EQUATIONS

We are now in a position to explicitly calculate the expectation value of the QCD Hamiltonian. For a quenched calculation, the pure gluonic part $\tilde{H}_{\mathrm{YM}}$ [Eq. (25)] can be ignored. We begin with the Dirac Hamiltonian $\bar{H}_{\mathrm{F}} = H_{\mathrm{F}}$ [Eq. (4)], whose expectation value reads

$$\langle H_{\mathrm{F}}\rangle = \int d^3x\int d^3y(-i\boldsymbol{\alpha}\boldsymbol{D})_{rs}\langle\psi_r^\dagger(\boldsymbol{x})\psi_s(\boldsymbol{y})\rangle, \tag{88}$$

where the covariant derivative is given in Eq. (6). Splitting the fermion field $\psi(\boldsymbol{x})$ into its positive and negative energy components, Eq. (41), one observes that only the expectation values $\langle\psi_+^{\dagger a}(\boldsymbol{x})\psi_+^b(\boldsymbol{y})\rangle$ and $\langle\psi_-^{\dagger a}(\boldsymbol{x})\psi_-^b(\boldsymbol{y})\rangle$ contribute to the kinetic energy of the quarks $\sim\boldsymbol{\alpha}\boldsymbol{p}$, while the coupling to the transverse gluons receives contributions from $\langle\psi_+^{\dagger a}(\boldsymbol{x})\psi_-^b(\boldsymbol{y})\rangle$ and $\langle\psi_-^{\dagger a}(\boldsymbol{x})\psi_+^b(\boldsymbol{y})\rangle$. One finds

$$\frac{\langle H_{\mathrm{F}}\rangle}{\delta^3(0)} = 2N_{\mathrm{C}}\int d^3p|\boldsymbol{p}|\frac{S^*(\boldsymbol{p})S(\boldsymbol{p})+R(\boldsymbol{p})-1}{1+S^*(\boldsymbol{p})S(\boldsymbol{p})+R(\boldsymbol{p})} + 2gN_{\mathrm{C}}C_F(2\pi)^3 \times\int đ^3p\int đ^3q\frac{V^*(\boldsymbol{p},\boldsymbol{q})+V(\boldsymbol{p},\boldsymbol{q})}{1+S^*(\boldsymbol{p})S(\boldsymbol{p})+R(\boldsymbol{p})}D(\boldsymbol{\ell})[1+(\hat{\boldsymbol{p}}\cdot\hat{\boldsymbol{\ell}})(\hat{\boldsymbol{q}}\cdot\hat{\boldsymbol{\ell}})], \tag{89}$$

where we have set $\boldsymbol{\ell}=\boldsymbol{p}-\boldsymbol{q}$. Furthermore, $C_{\mathrm{F}}=(N_C^2-1)/(2N_C)$ is the value of the quadratic Casimir in the fundamental representation and $D(\boldsymbol{p})=1/(2\omega(\boldsymbol{p}))$ is the Fourier transform of the gluon propagator (31). As is clear from the form of the Dirac Hamiltonian H_F (4), up to a constant the last term gives the condensate

$$\langle\psi^\dagger(\boldsymbol{x})\boldsymbol{\alpha}\cdot T_aA^a(\boldsymbol{x})\psi(\boldsymbol{x})\rangle.$$

To evaluate the energy density of $\bar{H}_{\mathrm{C}}^{\mathrm{F}}$ [Eq. (26)], we replace the Coulomb kernel $\hat{F}^{ab}(\boldsymbol{x},\boldsymbol{y})$ [Eq. (18)] by its gluonic expectation value, Eq. (35). This approximation is consistent with the quenched approximation and with the approximation (69) used for the kernels in the denominator of the quark propagator. One can easily convince oneself that within our approximation the coupling term $\bar{H}_{\mathrm{C}}^{\mathrm{coupl}}\sim\rho_{\mathrm{YM}}\rho_{\mathrm{F}}$ does not contribute, $\langle\bar{H}_{\mathrm{C}}^{\mathrm{coupl}}\rangle=0$. For this we notice that for a color diagonal gluon propagator, $\langle\rho_{\mathrm{YM}}\rangle_{\mathrm{G}}=0$. Furthermore, $\langle\rho_{\mathrm{F}}\rangle_{\mathrm{F}}$ contains within our approximation (69) at most terms linear in the gauge field A. Since ρ_{YM} is quadratic in the gauge field for the Gaussian Yang-Mills wave functional, it follows that $\langle\rho_{\mathrm{YM}}\langle\rho_{\mathrm{F}}\rangle_{\mathrm{F}}\rangle_{\mathrm{G}}=0$.

The expectation value of the Coulomb Hamiltonian $\bar{H}_{\mathrm{C}}^{\mathrm{F}}$, given by $\bar{H}_{\mathrm{C}}$ [Eq. (17)], with total color charge ρ^a replaced by the quark part ρ_{F}^a [Eq. (9)], is straightforwardly evaluated by splitting the fermion fields ψ, $\psi^\dagger$ into their positive and negative energy components, Eqs. (42) and (43), and applying Wick's theorem. The final form of the Coulomb energy density is

$$\frac{\langle\bar{H}_{\mathrm{C}}^{\mathrm{F}}\rangle}{\delta^3(0)} = \frac{1}{2}N_{\mathrm{C}}C_F(2\pi)^3\int đ^3pđ^3qV_{\mathrm{C}}(\boldsymbol{p}-\boldsymbol{q})[Y(\boldsymbol{p},\boldsymbol{q}) + Z(\boldsymbol{p},\boldsymbol{q})\hat{\boldsymbol{p}}\cdot\hat{\boldsymbol{q}}], \tag{90}$$

where we have introduced the abbreviations

$$Y(\boldsymbol{p},\boldsymbol{q}) = 1-\frac{S^*(\boldsymbol{p})S(\boldsymbol{q})+S(\boldsymbol{p})S^*(\boldsymbol{q})+S(\boldsymbol{p})S(\boldsymbol{q})+S^*(\boldsymbol{p})S^*(\boldsymbol{q})}{(1+S^*(\boldsymbol{p})S(\boldsymbol{p})+R(\boldsymbol{p}))(1+S^*(\boldsymbol{q})S(\boldsymbol{q})+R(\boldsymbol{q}))}, \tag{91a}$$

$$Z(\boldsymbol{p},\boldsymbol{q}) = -\frac{(1-S^*(\boldsymbol{p})S(\boldsymbol{p})-R(\boldsymbol{p}))(1-S^*(\boldsymbol{q})S(\boldsymbol{q})-R(\boldsymbol{q}))}{(1+S^*(\boldsymbol{p})S(\boldsymbol{p})+R(\boldsymbol{p}))(1+S^*(\boldsymbol{q})S(\boldsymbol{q})+R(\boldsymbol{q}))} + \frac{-S^*(\boldsymbol{p})S(\boldsymbol{q})-S(\boldsymbol{p})S^*(\boldsymbol{q})+S(\boldsymbol{p})S(\boldsymbol{q})+S^*(\boldsymbol{p})S^*(\boldsymbol{q})}{(1+S^*(\boldsymbol{p})S(\boldsymbol{p})+R(\boldsymbol{p}))(1+S^*(\boldsymbol{q})S(\boldsymbol{q})+R(\boldsymbol{q}))}. \tag{91b}$$

Note that $Y(\boldsymbol{p},\boldsymbol{q})$ and $Z(\boldsymbol{p},\boldsymbol{q})$ are both real. The vector kernel V enters the Coulomb energy density only through the loop integral $R(\boldsymbol{p})$ [Eq. (74)]. Putting $V(\boldsymbol{p},\boldsymbol{q})=0$, the loop integral $R(\boldsymbol{p})$ vanishes and the energy density (90) reduces to the expression obtained in Ref. [25] for the BCS-wave functional. Since the energy density given by Eqs. (89) and (90) is real, the variations with respect to S and S^* (or V and V^*) lead to complex conjugate equations, which can be shown to allow for real solutions. In the following, we therefore set $S(\boldsymbol{p})=S^*(\boldsymbol{p})$, $V(\boldsymbol{p},\boldsymbol{q})=V^*(\boldsymbol{p},\boldsymbol{q})$. The second term in $Z(\boldsymbol{p},\boldsymbol{q})$ [Eq. (91b)] then vanishes.

Minimizing the energy densities $\langle\bar{H}_{\mathrm{F}}\rangle$ [Eq. (89)] and $\langle\bar{H}_{\mathrm{C}}^{\mathrm{F}}\rangle$ [Eq. (90)] with respect to the variational kernels $S(\boldsymbol{k})$ and $V(\boldsymbol{k},\boldsymbol{k}')$, we obtain the following system of coupled integral equations:

$$S(\boldsymbol{k})=\frac{\frac{1}{2}C_F I_{\mathrm{C}}^{(1)}(\boldsymbol{k})}{|\boldsymbol{k}|-\frac{g}{2}C_F I_\omega(\boldsymbol{k})}, \tag{92}$$

$$V(\boldsymbol{k},\boldsymbol{k}')=-g\frac{1+S^2(\boldsymbol{k})+R(\boldsymbol{k})}{2|\boldsymbol{k}|-gC_F I_\omega(\boldsymbol{k})+C_F I_{\mathrm{C}}^{(2)}(\boldsymbol{k})}, \tag{93}$$

where we have introduced the loop integrals ($\ell=\boldsymbol{k}-\boldsymbol{q}$)

$$I_\omega(\boldsymbol{k})=2\int đ^3q V(\boldsymbol{k},\boldsymbol{q})D(\ell)[1+(\hat{\boldsymbol{k}}\cdot\hat{\ell})(\hat{\boldsymbol{q}}\cdot\hat{\ell})], \tag{94}$$

$$I_{\mathrm{C}}^{(1)}(\boldsymbol{k})=\int đ^3q\frac{V_{\mathrm{C}}(\boldsymbol{k}-\boldsymbol{q})}{1+S^2(\boldsymbol{q})+R(\boldsymbol{q})}[S(\boldsymbol{q})(1-S^2(\boldsymbol{k})+R(\boldsymbol{k}))-(\hat{\boldsymbol{k}}\cdot\hat{\boldsymbol{q}})S(\boldsymbol{k})(1-S^2(\boldsymbol{q})-R(\boldsymbol{q}))], \tag{95a}$$

$$I_{\mathrm{C}}^{(2)}(\boldsymbol{k})=\int đ^3q\frac{V_{\mathrm{C}}(\boldsymbol{k}-\boldsymbol{q})}{1+S^2(\boldsymbol{q})+R(\boldsymbol{q})}[2S(\boldsymbol{k})S(\boldsymbol{q})+(\hat{\boldsymbol{k}}\cdot\hat{\boldsymbol{q}})(1-S^2(\boldsymbol{q})-R(\boldsymbol{q}))]. \tag{95b}$$

Let us explain the notation of the loop integrals. The integrals with subscript C are the contributions from the color-Coulomb interaction, whereas I_ω refers to the transverse gluon interaction.

The gap equation (93) determines that the variational function $V(\boldsymbol{k},\boldsymbol{k}')$ depends on its first momentum argument only, i.e.,[2]

$$V(\boldsymbol{k},\boldsymbol{k}')=V(\boldsymbol{k}). \tag{96}$$

With this form of the vector kernel, the loop integrals $I_\omega(\boldsymbol{k})$ [Eq. (94)] and $R(\boldsymbol{k})$ [Eq. (74)] simplify to

$$I_\omega(\boldsymbol{k})=2V(\boldsymbol{k})I(\boldsymbol{k}),\qquad R(\boldsymbol{k})=C_F V^2(\boldsymbol{k})I(\boldsymbol{k}), \tag{97}$$

with

$$I(\boldsymbol{k})=\int đ^3qD(\ell)[1+(\hat{\boldsymbol{k}}\cdot\hat{\ell})(\hat{\boldsymbol{q}}\cdot\hat{\ell})],\quad \ell=\boldsymbol{k}-\boldsymbol{q}, \tag{98}$$

being the gluon loop. Then the system of coupled equations (92) and (93) becomes after the replacement $V(\boldsymbol{k})\to(-V(\boldsymbol{k}))$,[3]

$$S(\boldsymbol{k})=\frac{\frac{1}{2}C_F I_{\mathrm{C}}^{(1)}(\boldsymbol{k})}{|\boldsymbol{k}|+gC_F V(\boldsymbol{k})I(\boldsymbol{k})}, \tag{99}$$

$$V(\boldsymbol{k})=\frac{g}{2}\frac{1+S^2(\boldsymbol{k})+R(\boldsymbol{k})}{|\boldsymbol{k}|+gC_F V(\boldsymbol{k})I(\boldsymbol{k})+\frac{1}{2}C_F I_{\mathrm{C}}^{(2)}(\boldsymbol{k})}. \tag{100}$$

Once these equations are solved, the quark part of the vacuum wave functional of QCD is known and all quark observables can, in principle, be evaluated. These equations need the gluon propagator (31) and the non-Abelian Coulomb potential (35) as input. For the gluon propagator, we will use the Gribov formula (33). Following Ref. [25] for the Coulomb potential, we use the confining form (36), which in momentum space reads

$$V_{\mathrm{C}}(\boldsymbol{k})=\frac{8\pi\sigma_{\mathrm{C}}}{\boldsymbol{k}^4}. \tag{101}$$

With this potential, the Coulomb loop integrals $I_{\mathrm{C}}^{(1)}(\boldsymbol{k})$ [Eq. (95a)] and $I_{\mathrm{C}}^{(2)}(\boldsymbol{k})$ [Eq. (95b)] are UV finite. Then the only UV-divergent quantity occurring in the gap equations is the gluon loop integral $I(\boldsymbol{k})$ [Eq. (98)].

The gluon energy (33) contains a mass scale (Gribov mass) M_{G} which separates the UV and IR regions of the gluon propagator. To isolate the divergencies of $I(\boldsymbol{k})$, we replace the gluon propagator in the momentum regime $q>M_{\mathrm{G}}$ by its UV part

$$D_{\mathrm{UV}}(\boldsymbol{k})=1/(2|\boldsymbol{k}|), \tag{102}$$

and define the UV part of the gluon loop integral as

$$I_{\mathrm{UV}}(\boldsymbol{k})=\int\frac{d^3q}{(2\pi)^3}D_{\mathrm{UV}}(\boldsymbol{k}-\boldsymbol{q})\Theta(|\boldsymbol{q}|-M_{\mathrm{G}})\times[1+(\hat{\boldsymbol{k}}\cdot\hat{\ell})(\hat{\boldsymbol{q}}\cdot\hat{\ell})],\qquad \ell=\boldsymbol{k}-\boldsymbol{q}. \tag{103}$$

The Θ function ensures that only loop momenta q larger than the Gribov mass scale M_{G} contribute. Introducing a momentum cutoff Λ, this integral is readily evaluated. Separating divergent and finite pieces

$$I_{\mathrm{UV}}(\boldsymbol{k},\Lambda)=I_{\mathrm{UV}}^{\mathrm{fin}}(\boldsymbol{k})+I_{\mathrm{UV}}^{\mathrm{div}}(\boldsymbol{k},\Lambda), \tag{104}$$

we find

$$I_{\mathrm{UV}}^{\mathrm{div}}(k,\Lambda)=\frac{1}{8\pi^2}\left(\Lambda^2-\frac{2}{3}\Lambda k\right), \tag{105}$$

[2]In an unquenched calculation, taking the variation of the pure Yang-Mills part $\bar{H}_{\mathrm{YM}}^{C}$ [Eq. (25)] into account, this statement no longer holds true.

[3]By the definition of V [see Eqs. (50), (51), and (54)], this replacement is equivalent to changing the sign of the gauge field $\boldsymbol{A}(\boldsymbol{x})$ or of the coupling constant g, which leaves the theory invariant.

and

$$I_{\rm UV}^{\rm fin}(k) = \frac{1}{8\pi^2}\left[\left(-M_{\rm G}^2 + \frac{2}{3}kM_{\rm G}\right)\Theta(M_{\rm G}-k) + \left(-\frac{2}{3}\frac{M_{\rm G}^3}{k} + \frac{1}{6}\frac{M_{\rm G}^4}{k^2} + \frac{1}{6}k^2\right)\Theta(k-M_{\rm G})\right]. \quad (106)$$

Note that the UV-divergent part $I_{\rm UV}^{\rm div}(k)$ [Eq. (105)] is independent of the Gribov mass scale $M_{\rm G}$, which was used to define the UV regime. A comment is here in order: a shift of the integration variable $q \to l$ would make the integral a (diverging) constant independent of k. However, as is well known, shifting the integration variable before regularization changes the value of the regularized integral. It is important to keep the rooting as in Eq. (103) for which the UV-finite part of the gluon loop integral, $I_{\rm UV}^{\rm fin}(k)$ [Eq. (106)] has the asymptotic behavior

$$I_{\rm UV}^{\rm fin}(k\to\infty) = \frac{k^2}{48\pi^2}, \quad (107)$$

which ensures that the dressing function $V(\boldsymbol{k})$ has the correct UV-perturbative behavior, as we will see in the next section.

We now define the regularized part of the gluon loop integral (98) by subtracting its UV-divergent piece $I_{\rm UV}^{\rm div}(\boldsymbol{k},\Lambda)$

$$I_{\rm reg}(k) = \lim_{\Lambda\to\infty}[I(k,\Lambda) - I_{\rm UV}^{\rm div}(k,\Lambda)] + C, \quad (108)$$

where C is an arbitrary finite renormalization constant. In principle, this constant could be determined by minimizing the energy density. This would, however, require us to renormalize not only the gap equations (99) and (100), but also the energy density itself, which is quite involved and which we have not done yet. However, we can circumvent this problem by noticing that the quark condensation occurs in order to lower the energy of the system. (The superconducting groundstate has a lower energy than the normal state.) We can therefore assume to minimize the energy density by maximizing the quark condensate.

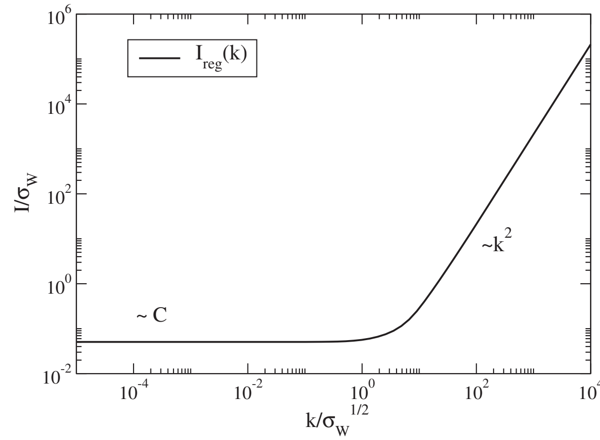

FIG. 2. Regularized loop integral $I_{\rm reg}(k)$ in units of the string tension $\sqrt{\sigma_{\rm W}}$, with $M_{\rm G}$ given in Eq. (34).

Hence, we will choose C so as to maximize the magnitude of the quark condensate. We have found that the optimal value is $C = M_{\rm G}^2/(8\pi^2)$. The regularized gluon loop integral (108) is plotted in Fig. 2.

VIII. ASYMPTOTIC ANALYSIS

Below we analyze the coupled equations (99) and (100) in the IR and UV. For this purpose we analyze first the loop integrals $I_{\rm C}^{(1)}(\boldsymbol{k})$ [Eq. (95a)], $I_{\rm C}^{(2)}(\boldsymbol{k})$ [Eq. (95b)], and $I(\boldsymbol{k})$ [Eq. (98)].

The angular parts of the Coulomb integrals $I_{\rm C}^{(1)}(\boldsymbol{k})$ and $I_{\rm C}^{(2)}(\boldsymbol{k})$ can be reduced to the following two types of angular integrals:

$$\int d\Omega_q V_{\rm C}(\boldsymbol{k}-\boldsymbol{q}), \qquad \int d\Omega_q V_{\rm C}(\boldsymbol{k}-\boldsymbol{q})\hat{\boldsymbol{k}}\cdot\hat{\boldsymbol{q}}, \quad (109)$$

where $\int d\Omega_q = \int_0^\pi \sin\theta d\theta \int_0^{2\pi} d\varphi$ and $\hat{\boldsymbol{k}}\cdot\hat{\boldsymbol{q}} = \cos\theta$. The φ integral is trivial. For the Coulomb potential (101), the integrals over $z = \cos\theta$ can also be taken analytically, using

$$L(k,q) \equiv \int_{-1}^{1} dz \frac{1}{(k^2 - 2kqz + q^2)^2} = \frac{2}{(k^2-q^2)^2}, \quad (110a)$$

$$M(k,q) \equiv \int_{-1}^{1} dz \frac{z}{(k^2 - 2kqz + q^2)^2} = \frac{k^2+q^2}{kq(k^2-q^2)^2} + \frac{1}{2}\frac{1}{k^2q^2}\ln\left|\frac{k-q}{k+q}\right|. \quad (110b)$$

A. IR analysis

We first study the IR behavior by expanding the kernels $L(k,q)$ [Eq. (110a)] and $K(k,q)$ [Eq. (110b)] in powers of k, yielding

$$L(k,q) = \frac{2}{q^4} + \frac{4k^2}{q^6} + \mathcal{O}(k^4), \quad (111)$$

$$M(k,q) = \frac{8}{3}\frac{k}{q^5} + \mathcal{O}(k^3). \quad (112)$$

For $k\to 0$ the leading contribution comes from the kernel $L(k,q)$, while the kernel $M(k,q)$ vanishes at this order. For vanishing momenta, the (regularized) integral $I(k)$ [Eq. (108)] is IR finite. Assuming the variational functions $S(k)$, $V(k)$ to be analytic in the IR region, the gap equation (99) for $S(k)$ reduces for $k\to 0$ to

$$gC_F V(0)I(0)S(0) = \tilde{I}_C^{(1)}(0), \tag{113}$$

where

$$\tilde{I}_C^{(1)}(0) = [1 - S^2(0) + C_F V^2(0)I(0)]I_C^{IR}(0) \tag{114}$$

and we have introduced the abbreviation[4]

$$I_C^{IR}(0) = G\int dq q^2 L(k=0,q)\frac{S(q)}{1+S^2(q)+R(q)}, \tag{115}$$

with $L(k,q)$ given in Eq. (111) and $G = \sigma_C/\pi$. Equation (113) is a quadratic equation and can be solved as

$$S(0) = \frac{-gC_F V(0)I(0) \pm \sqrt{(gC_F V(0)I(0))^2 + 4(I_C^{IR}(0))^2(1 + C_F V^2(0)I(0))}}{2I_C^{IR}(0)}. \tag{116}$$

For the BCS type of wave functional, defined by Eq. (50) with vanishing vector kernel $V(k)$, Eq. (113) simplifies to

$$0 = [1 - S^2(0)]I_C^{IR}(0) \tag{117}$$

and is solved for $S(k\to 0) = \pm 1$. This solution is of course also obtained from Eq. (116) with $V(0) = 0$. With the coupling of the quarks to the transverse gluons included $[V(k)\neq 0]$, *all* parts of the QCD energy contribute to the infrared value $S(0)$ of the scalar gap function $S(k)$, which is then no longer constrained to ± 1.[5] To find the infrared value of $V(k)$, we take the $k\to 0$ limit of Eq. (100), which yields

$$[gC_F V(0)I(0) + \tilde{I}_C^{(2)}(0)]V(0) = \frac{g}{2}[1 + S^2(0) + C_F V^2(0)I(0)], \tag{118}$$

with $\tilde{I}_C^{(2)}(0) = 2S(0)I_C^{IR}(0)$ and $I_C^{IR}(0)$ defined by Eq. (115). Equation (118) can be solved for $V(0)$, yielding

$$V(0) = \frac{-2S(0)I_C^{IR} \pm \sqrt{(2S(0)I_C^{IR})^2 + (gC_F I(0))(g(1 + S^2(0)))}}{gC_F I(0)}. \tag{119}$$

Like $S(k)$, the vector kernel $V(k)$ is IR finite. Since $V(k=0)\neq 0$, we can expect that the coupling of the quarks to the transverse gluons is indeed relevant for the infrared physics.

B. UV analysis

Due to asymptotic freedom, we expect the coupling kernels $S(\boldsymbol{k})$ and $V(\boldsymbol{k})$ to vanish for $k\to\infty$. Therefore, we make the following power-law *Ansätze*

$$S(k\to\infty) = \frac{A}{k^\alpha}, \qquad V(k\to\infty) = \frac{B}{k^\beta}. \tag{120}$$

Since the integrals $L(k,q)$, $M(k,q)$ [Eqs. (110a) and (110b)] are symmetric in the two entries k and q, the UV behavior of these integrals for large $k\to\infty$ can be obtained from the IR expressions for $k\to 0$ [Eqs. (111) and (112)] by interchanging the momenta $k\leftrightarrow q$, yielding

$$L(k,q) = \frac{2}{k^4} + \mathcal{O}\left(\frac{1}{k^6}\right), \tag{121}$$

$$M(k,q) = \frac{8q}{3k^5} + \mathcal{O}\left(\frac{1}{k^7}\right). \tag{122}$$

With these expressions one finds for the UV behavior of the Coulomb integrals (94) and (95a)

$$I_C^{(1)}(k\to\infty) = \left(\frac{2}{k^4} + O\left(\frac{1}{k^6}\right)\right)[1 - S(k) + C_F V^2(k)I(k)]I_C^{UV} \tag{123a}$$

$$I_C^{(2)}(k\to\infty) = \left(\frac{2}{k^4} + O\left(\frac{1}{k^6}\right)\right)2S(k)I_C^{UV}, \tag{123b}$$

with

$$I_C^{UV} = G\int dq q^2 \frac{S(q)}{1+S^2(q)+R(q)}. \tag{124}$$

Furthermore, the finite UV leading term of the gluon loop integral $I(k)$ [Eq. (94)] is given by $I_{UV}^{fin}(k)\sim k^2$; see Eq. (107).

With the UV behavior of the loop integrals at hand, it is now straightforward to carry out the UV analysis of the gap equations (98) and (99). One finds the following behavior:

[4]We note that the integral $I_C^{IR}(0)$ is finite when the infrared regulator ε [Eq. (133)] is introduced, which is done in the numerical evaluation.

[5]However, using a perturbative gluon propagator, i.e., $\omega_{UV}(\boldsymbol{k}) = |\boldsymbol{k}|$, the infrared value of S is, as for the BCS case, constrained to be unity [since the loop integral $I(k)$ [Eq. (98)] then vanishes like k^2 for small momenta].

$$S(k) \sim 1/k^5, \qquad V(k) \sim 1/k, \qquad k \to \infty. \tag{125}$$

The same UV behavior of $S(k)$ was found in Ref. [25].

The results obtained in this chapter in the IR and UV analysis are all confirmed in the numerical solution of the gap equations (99) and (100). The variational functions show a perfect power-law behavior for large momenta; see Fig. 4.

IX. CHIRAL SYMMETRY BREAKING WITH SPATIAL GLUONS ONLY?

We first explore whether, neglecting the Coulomb potential $V_C(\boldsymbol{k})$ [Eq. (101)], the coupling of the quarks to the transverse gluons alone can generate spontaneous breaking of chiral symmetry.

Neglecting the Coulomb potential implies $I_C^{(1,2)}(k) = 0$ [Eqs. (95a) and (95b)] and simplifies the equations of motion (99) and (100) to

$$S(k)(k + gC_F V(k)I(k)) = 0 \tag{126}$$

$$V(k) = \frac{g}{2}\,\frac{1 + S^2(k) + C_F V^2(k)I(k)}{k + gC_F V(k)I(k)}. \tag{127}$$

A nonvanishing quark condensate (87) requires $S(k) \neq 0$, for which Eq. (126) reduces to

$$k + gC_F V(k)I(k) = 0. \tag{128}$$

This equation has no solution, in particular for $k = 0$, since $I(k = 0) \neq 0$. Hence, with the neglect of the color Coulomb potential $V_C(\boldsymbol{k})$ [Eq. (101)], only the trivial solution $S(k) = 0$ exists; i.e., spontaneous breaking of chiral symmetry does not occur.

For the trivial solution $S(k) = 0$ of the gap equation (99), the equation (100) for the vector kernel reduces to

$$V(\boldsymbol{k}) = \frac{g}{2}\,\frac{1 + C_F V^2(\boldsymbol{k})I(\boldsymbol{k})}{|\boldsymbol{k}| + gC_F V(\boldsymbol{k})I(\boldsymbol{k})}, \tag{129}$$

which can be easily solved, yielding

$$V(k) = \frac{k}{gC_F I(k)}\left[\pm\sqrt{1 + \frac{g^2 C_F I(k)}{k^2}} - 1\right]. \tag{130}$$

Only the upper sign corresponds to the physical solution, since the vector kernel $V(k)$ has to vanish in the limit $g \to 0$. Indeed for the upper sign we find, for small g with the UV behavior of the gluon loop $I(k)$ [Eq. (107)],

$$V(k) = \frac{g}{2k} + O\left(\left(\frac{g}{k}\right)^2\right). \tag{131}$$

We also observe from the solution (130) that the limit of small g is equivalent to the limit of large k, which is, of course, a consequence of asymptotic freedom. Thus, Eq. (131) already gives the UV behavior of $V(k)$. The solution (130) provides also an IR constant behavior as found in the previous section:

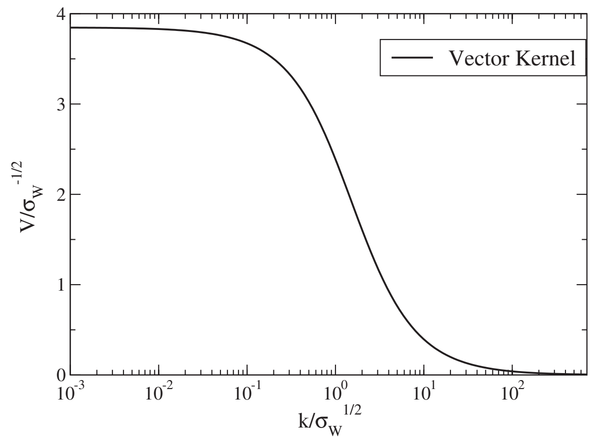

FIG. 3. The vector kernel $V(k)$ resulting from the solution of the gap equation (131).

$$V(k = 0) = \frac{1}{\sqrt{C_F I(0)}} = \text{const.} \tag{132}$$

The solution $V(k)$ [Eq. (130)] is plotted in Fig. 3. All dimensionful quantities are given in units of the Wilsonian string tension $\sigma_W = (440\ \text{MeV})^2$. In the present calculation, the physical scale is set by the Gribov mass M_G (34), which enters the gluon energy (33). For the Casimir invariant C_F, the $SU(3)$ value $C_F = 4/3$ is taken. Moreover, the (running) coupling g (which was calculated in the Hamiltonian approach in Ref. [5] from the ghost-gluon vertex) is replaced by its infrared value $g \equiv g(k = 0) = 8\pi/\sqrt{3N_C}$.

The investigations of the present section show that the coupling of the quarks to the transverse (spatial) gluons alone is incapable of inducing spontaneous breaking of chiral symmetry. On the other hand, we know from Ref. [25] that the color Coulomb interaction $V_C(\boldsymbol{k})$ [Eq. (101)] alone does generate spontaneous breaking of chiral symmetry but not the sufficient amount, as we will see in the next section.

X. NUMERICAL RESULTS

When the Coulomb potential $V_C(\boldsymbol{k})$ [Eq. (101)] is included, the equations of motion (99) and (100) contain two dimensionful quantities: the Coulomb string tension σ_C [Eq. (37)] and the Gribov mass M_G [Eq. (33)] of the transverse gluon propagator. As discussed at the end of Sec. III, these two quantities are not independent of each other. The Gribov mass M_G can be rather accurately determined on the lattice and we will use its lattice value (34). The Coulomb string tension is much less accurately determined; see Eq. (37).

For the numerical solution of the coupled equations (99) and (100), all dimensionful quantities are expressed in terms of the Coulomb string tension σ_C. Furthermore, to

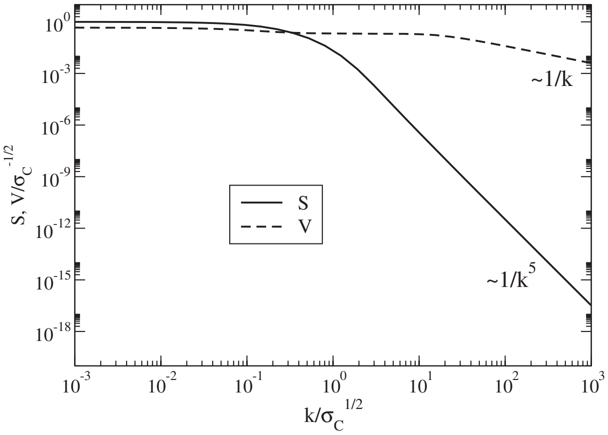

FIG. 4. Variational kernels S (full curve) and V (dashed curve) solving the gap equations (99) and (100).

avoid problems due to the divergence of the Coulomb potential $V_C(\boldsymbol{k})$ at $\boldsymbol{k} \longrightarrow 0$, we introduce an IR regulator ε

$$V_C(\boldsymbol{k}) \longrightarrow V_C(\boldsymbol{k}, \varepsilon) = \frac{8\pi\sigma_C}{\boldsymbol{k}^2(\boldsymbol{k}^2 + \varepsilon^2)}. \tag{133}$$

Then our solutions $S(\boldsymbol{k})$ and $V(\boldsymbol{k})$ will depend on ε. However, we have tested that the solutions $S(\boldsymbol{k}, \varepsilon)$ and $V(\boldsymbol{k}, \varepsilon)$ both converge for $\varepsilon \longrightarrow 0$. The resulting numerical solutions for $S(k)$ and $V(k)$ are shown in Fig. 4. These solutions confirm the asymptotic behavior obtained in Sec. VIII. From these solutions one finds the dynamical quark mass $M(k)$ [Eq. (85)], shown in Fig. 5. It reaches a plateau value at small momenta and vanishes for $k \longrightarrow \infty$, in accordance with asymptotic freedom. The plateau value $M(k = 0)$ defines the constituent mass, which is obtained as

$$M(0) = 132\ \mathrm{MeV}\sqrt{\sigma_C/\sigma_W}. \tag{134}$$

For the quark condensate, Eq. (87), we find

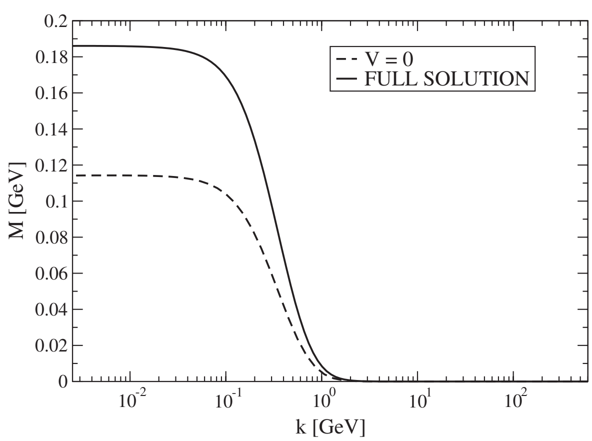

FIG. 5. The dynamical quark mass $M(\boldsymbol{k})$ [Eq. (85)] for the full solution and for $V = 0$ with $\sigma_C = 2\sigma_W$.

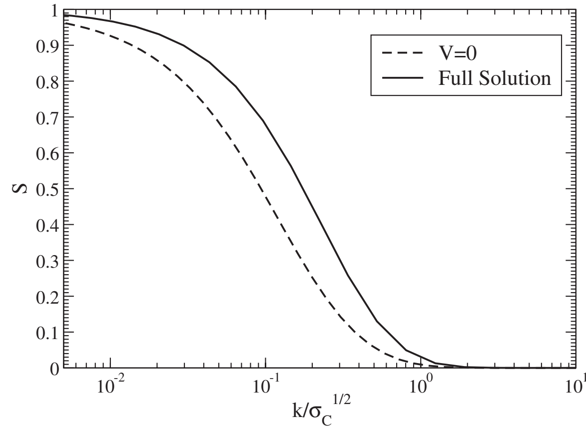

FIG. 6. Variational kernel S comparing the solutions with $V = 0$ and $V \neq 0$.

$$\langle\bar{\psi}\psi\rangle \simeq (-135\ \mathrm{MeV}\sqrt{\sigma_C/\sigma_W})^3. \tag{135}$$

Using $\sigma_C = (2\ldots 3)\sigma_W$, we obtain

$$M(0) \simeq (186\ldots 230)\ \mathrm{MeV} \tag{136}$$
$$\langle\bar{\psi}\psi\rangle \simeq -(191\ldots 234\ \mathrm{MeV})^3.$$

While the obtained mass is somewhat smaller than the constituent mass of the light quark flavors, which is about 300 MeV, the obtained chiral condensate compares more favorably with the phenomenological value of $\langle\bar{\psi}\psi\rangle = (-230\ \mathrm{MeV})^3$.

Let us now compare our results with those obtained when the coupling of the quarks to the transverse gluons is neglected, $V(k) = 0$, i.e., when the BCS-type quark wave functional is used, Ref. [25]. Figures 5 and 6 show the dynamical mass $M(\boldsymbol{k})$ and the scalar form factor $S(\boldsymbol{k})$, respectively, for both cases. When the coupling to the

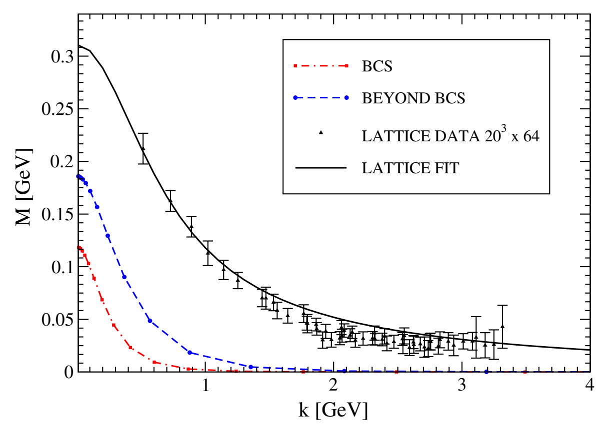

FIG. 7 (color online). The dynamical quark mass $M(k)$ [Eq. (85)] for $\sigma_C = 2\sigma_W$ and $\sqrt{\sigma_W} = 440$ MeV compared to the lattice data obtained in Ref. [42]. The dashed curve is obtained with the quark-gluon coupling included in the wave functional, while the dotted curve is obtained with the BCS wave functional.

transverse gluons is neglected, both $M(\boldsymbol{k})$ and $S(\boldsymbol{k})$ are substantially reduced. One finds then

$$M(0) \simeq 84\ \mathrm{MeV}\sqrt{\sigma_{\mathrm{C}}/\sigma_{\mathrm{W}}}$$
$$\langle \bar{\psi}\psi \rangle \simeq -(113\ \mathrm{MeV}\sqrt{\sigma_{\mathrm{C}}/\sigma_{\mathrm{W}}})^3. \tag{137}$$

Compared to these results, the inclusion of the coupling of the quarks to the transverse gluons, i.e., of the vector kernel $V(k)$, increases the quark condensate $\langle \bar{\psi}\psi \rangle$ [Eq. (135)] by 20% and the constituent mass [Eq. (134)] by 60%.

In Fig. 7 we compare our results for the dynamical mass to the lattice data obtained recently in Ref. [42]. As one observes the shape of the momentum, dependence is reproduced but the absolute values are still too small.

XI. UNQUENCHING THE GLUON PROPAGATOR

So far all calculations were done in the quenched approximation; i.e., the gluon propagator and the Coulomb kernel were taken from the pure Yang-Mills sector and used as input for the treatment of the quark sector. In a fully unquenched calculation, the variation would be carried out at the same time with respect to all variational kernels and the resulting equations of motion had to be solved self-consistently. Below we give an estimate of the unquenching effects by calculating the corrections to the gluon propagator but using in these corrections the quenched gluon propagator as input.

The unquenching arises from two sources: first, from those fermionic contributions to the energy density, which depend on the gluon propagator [see Eqs. (89) and (90)], and second, from the norm of the fermionic wave functional (the fermion determinant) [see Eq. (63)], which does depend on the gauge field. In a fully unquenched calculation, the fermionic wave functional must not be normalized separately from the gluonic one, as we did in the present calculation given above. We will investigate both effects separately.

A. Quark energy contributions

In Ref. [14] it was shown that the gluonic Coulomb term is irrelevant for the Yang-Mills sector. We expect that this is also true for the contribution of the quark Coulomb energy (90) to the unquenching of the gluon propagator. This is because the Coulomb potential (35) depends only implicitly on the gluon propagator, and variation of Eq. (90) with respect to the gluon propagator gives rise to more than two loops. We are then left with the quark energy $\langle H_F \rangle$ [Eq. (89)]. Variation of this quantity with respect to the gluon propagator $\omega^{-1}(\boldsymbol{k})$ yields

$$\begin{aligned}\frac{\delta}{\delta\omega^{-1}(\boldsymbol{k})}\left[\frac{\langle H_F\rangle}{\delta^3(0)}\right] &\equiv \Delta(\boldsymbol{k})\\ &= N_C C_F \int d^3p \frac{1}{1+S^*(\boldsymbol{p})S(\boldsymbol{p})+R(\boldsymbol{p})}\left[g(V^*(\boldsymbol{p},\ell)+V(\boldsymbol{p},\ell)) + 2\frac{V(\boldsymbol{p},\ell)V^*(\ell,\boldsymbol{p})}{1+S^*(\boldsymbol{p})S(\boldsymbol{p})+R(\boldsymbol{p})}\right]\\ &\quad\times[1+(\hat{\boldsymbol{p}}\cdot\hat{\boldsymbol{k}})(\hat{\ell}\cdot\hat{\boldsymbol{k}})],\end{aligned} \tag{138}$$

with $\ell = \boldsymbol{p} - \boldsymbol{k}$. This gives an extra contribution to the gluonic gap equation, Ref. [1], which then reads

$$\omega^2(\boldsymbol{k}) = \omega^2_{\mathrm{YM}}(\boldsymbol{k}) + \Delta(\boldsymbol{k}), \tag{139}$$

where $\omega_{\mathrm{YM}}(\boldsymbol{k})$ is the gluon energy in the pure Yang-Mills case [in the previous section this quantity was called $\omega(\boldsymbol{k})$]. Obviously, the unquenching correction $\Delta(\boldsymbol{k})$ [Eq. (138)] disappears when the coupling of the quarks to the transverse gluons is neglected, $V(\boldsymbol{p},\ell) = 0$.

The quark contribution $\Delta(\boldsymbol{k})$ [Eq. (138)] is UV divergent. It is straightforward to extract its divergence structure

$$\Delta_{\mathrm{DIV}}(k,\Lambda) = \sim\Lambda^2 + \sim\Lambda + \sim k^2 \ln\Lambda, \tag{140}$$

where Λ is the 3-momentum cutoff. The quadratic and linear divergence disappear when the gap equation is renormalized by subtracting it at a renormalization scale. More elegantly these terms, as well as the logarithmic divergence, are eliminated by adding appropriate counterterms to H_{F} [Eq. (4)], analogous to the renormalization in the gluon sector; see Refs. [8,43]. Here we will just consider the finite part of $\Delta(\boldsymbol{k})$ [Eq. (138)], use the renormalization condition

$$\frac{\omega^2(\zeta,\Lambda)}{\zeta^2} = \frac{\omega^2_{\mathrm{YM}}(\zeta)}{\zeta^2}, \tag{141}$$

and fix the renormalization point ζ in the ultraviolet, which is justified since for large momenta the quark vacuum becomes bare.

To estimate the unquenching effect due to the quark energy contribution we assume for $\omega_{\mathrm{YM}}(k)$ the Gribov formula (33) with the same Gribov mass $M_{\mathrm{G}} = 880\,\mathrm{MeV}$ as used above. The resulting gluon propagator $D(k) = 1/(2\omega(k))$ is shown in Fig. 8 together with the quenched result. It is seen that the unquenching decreases the gluon propagator in the mid-momentum regime but leaves the UV and IR asymptotic behavior unchanged. Unfortunately, it is the mid-momentum regime which is relevant for the hadron physics and also for the deconfinement phase transition. Therefore, unquenching seems to be important for a

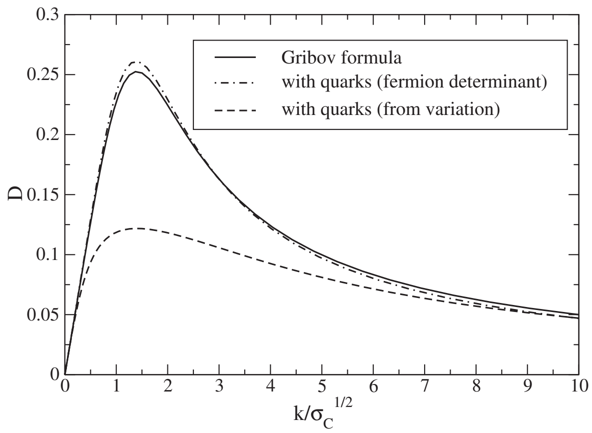

FIG. 8. The full curve is the Gribov form. The dash-dotted curve is the unquenching effect considered in Eq. (139). The dashed line shows the result (147).

realistic description of hadrons and the deconfinement transition.

B. The fermion determinant

As already discussed above, in a fully unquenched calculation only the total wave functional of QCD can be normalized while the norm of the quark wave functional becomes a dynamical object due to its dependence on the gauge field. The norm of our quark wave functional (50) is given by Eq. (63):

$$\langle \phi_{\mathrm{F}} | \phi_{\mathrm{F}} \rangle = \mathrm{Det}\Omega = \exp(\mathrm{Tr}\ln\Omega), \tag{142}$$

where the matrix Ω is defined by Eq. (62) and is a functional of the gauge field $\boldsymbol{A}$. By Wick's theorem, this quantity arises as a factor in all fermionic expectation values. In the scalar product of the QCD wave functionals (22), $\mathrm{Det}\Omega$ can be considered as part of the Yang-Mills wave functional $|\phi_{\mathrm{YM}}(\boldsymbol{A})|^2$. To keep the gluonic functional integral Gaussian, we expand $\mathrm{Tr}\ln\Omega$ up to second order in the gauge field. With [see Eqs. (51) and (62)]

$$\Omega = \Omega_0 + \Omega_1 \cdot A, \tag{143}$$

this yields

$$\begin{aligned}\mathrm{Tr}\ln\Omega &= \mathrm{Tr}\ln\Omega_0 + \mathrm{Tr}(\Omega_0^{-1}\Omega \cdot A) \\ &\quad - \frac{1}{2}\mathrm{Tr}(\Omega_0^{-1}\Omega_1 \cdot A\Omega_0^{-1}\Omega_1 \cdot A) \\ &= \mathrm{const} + \frac{1}{2}\int A\Sigma A. \end{aligned} \tag{144}$$

The zeroth order term is an irrelevant constant which can be absorbed into the overall normalization of the QCD wave functional. The linear term vanishes due to the color trace, while the quadratic term gives the quark loop contribution Σ to the gluon self-energy. Due to the transversality of the gauge field and the absence of external color fields, we have

$$\Sigma_{ij}^{ab}(\boldsymbol{k}) = \delta^{ab} t_{ij}(\boldsymbol{k})\Sigma(\boldsymbol{k}). \tag{145}$$

The explicit calculation yields

$$\begin{aligned}\Sigma(\boldsymbol{k}) = -\frac{1}{2}\int đ^3 p \frac{V^2(\boldsymbol{p}, \boldsymbol{p}+\boldsymbol{k})}{(1+S^2(\boldsymbol{p}+\boldsymbol{k}))(1+S^2(\boldsymbol{p}))} \\ \times (1 + S(\boldsymbol{p})S(\boldsymbol{p}+\boldsymbol{k}))(1 + (\hat{\boldsymbol{k}}\cdot\hat{\boldsymbol{p}}) \\ \times (\hat{\boldsymbol{k}} \cdot (\widehat{\boldsymbol{p}+\boldsymbol{k}}))).\end{aligned} \tag{146}$$

Taking into account the unquenching effects from the quark loop, the gluon propagator is then given by

$$\omega(\boldsymbol{k}) = \omega_{\mathrm{YM}}(\boldsymbol{k}) + \Sigma(\boldsymbol{k}). \tag{147}$$

Again the unquenching disappears, $\Sigma(\boldsymbol{k}) = 0$, when the coupling of the quarks to the spatial gluons is switched off in the wave functional, $V(\boldsymbol{k}) = 0$. The integral $\Sigma(\boldsymbol{k})$ [Eq. (146)] is linearly divergent. Carrying out the renormalization as in the previous subsection, we find for the (partially) quenched gluon propagator the result shown in Fig. 8. Again, the gluon propagator is affected by the quarks only in the intermediate momentum region. However, now the propagator is increased, although the amount of increase is much less than the decrease found in the previous subsection from the quark-gluon coupling energy $\langle H_F \rangle$ [Eq. (138)]. From this we can conclude that the unquenching reduces the gluon propagator in the mid-momentum regime. In a self-consistent solution, both of these unquenching effects combine nontrivially in the gap equations. Due to the net reduction of the gluon propagator by the unquenching, we expect that in a fully self-consistent calculation, the unquenching effects are less dramatic than found above but may still be essential.

XII. SUMMARY AND CONCLUSIONS

The variational approach to Yang-Mills theory in Coulomb gauge developed previously in Ref. [1] has been extended to full QCD. The QCD Schrödinger equation has been variationally solved in the quenched approximation using an *Ansatz* for the quark wave functional, which explicitly includes the coupling of the quarks to the spatial gluons and thus goes beyond previously used BCS-type quark wave functionals. For the Yang-Mills sector, we have used the vacuum wave functional determined previously in [1,5] as input.

Our quark wave functional contains two variational kernels: one scalar kernel $S(\boldsymbol{k})$, which is related to the quark condensate and occurs already in the BCS-type wave functionals, and a vector kernel $V(\boldsymbol{k})$, which represents the form factor of the quark gluon coupling. The equations of motion following from the variational principle for these kernels have been solved analytically in the infrared, in the ultraviolet, and numerically in the whole momentum regime. Both kernels are infrared finite and vanish at large momenta in accordance with asymptotic freedom. We have shown that neglecting the color

Coulomb potential, the coupling of the quarks to the spatial gluons is not capable of triggering spontaneous breaking of chiral symmetry and always produces a vanishing scalar kernel $S(\boldsymbol{k}) = 0$. When the confining color Coulomb potential is included, the coupling of the quarks to the gluons substantially enhances the amount of chiral symmetry breaking towards the phenomenological findings. The quark condensate is increased by about 20% and compares favorably with the phenomenological values. Although the constituent quark mass is increased by about 60% due to the coupling of the quarks to the spatial gluons, the value found is still somewhat small.

One may speculate where the missing chiral strength is lost in the present approach. Certainly we have used a couple of approximations but given the success of the present approach in the pure Yang-Mills sector, one would perhaps expect a better agreement with the phenomenological data. First one should remark that the lattice calculations done in Coulomb gauge, Ref. [42], show that the running quark mass $M(\boldsymbol{k})$ is smaller in the quenched calculation compared to the dynamical one. But this effect is only of the order of a few percent. Next one may question the additional approximation $1/(\mathbb{1} + K\bar{K}) \to 1/(\mathbb{1} + \langle K\bar{K}\rangle_{\mathrm{G}})$ we have used in the quark sector when calculating the gluonic expectation values of fermionic operators. We do not expect that this approximation makes big quantitative changes, since this replacement is exact for the scalar kernel $K_0 \sim S(\boldsymbol{k})$, which dominates the chiral properties. One may then ponder on our *Ansatz* for the quark wave functional, Eq. (50). This wave functional, being given by an exponent which is bilinear in the quark field, represents the most general Slater determinant. One certainly does not want to abandon the determinantal states in order not to lose Wick's theorem. However, we have assumed for the kernel K in the exponent of the quark wave functional an expansion in powers of the gauge field and restricted this expansion in linear order. This is certainly a rather crude approximation. It is straightforward to extend the present approach by keeping in the kernel K (51) higher powers of the spatial gluon field. Then the fermionic part of the present calculation does not change at all. What changes is the gluonic expectation value, which, however, can be done by using Wick's theorem since the employed gluonic wave functional is Gaussian. We expect a substantial improvement by including terms in the kernel K, which are second order in the gauge field. This will introduce further variational kernels, which can only improve the results towards the exact ones. Let us also mention that one may also include a quark-gluon coupling term of the type used in the present paper [see Eq. (54)] with the Dirac matrix $\boldsymbol{\alpha}$ replaced by the Nabla operator.

In principle, one can go beyond the determinantal quark wave functional (50) and include in its exponent, e.g., four-fermion operators. Such a wave functional can be handled by means of the approach based on Dyson-Schwinger equation techniques and developed in Ref. [36] for the treatment of non-Gaussian wave functionals in the Yang-Mills sector. An extension of this approach to full QCD is in progress [44].

Finally in the last part of our paper we have considered a partial unquenching by including the change of the gluonic energy due to the presence of the quarks. Our results show that unquenching reduces the static gluon propagator in the mid-momentum regime. The unquenching effects disappear when the coupling of the quarks to the spatial gluons is neglected.

Some results of the present paper were used in Ref. [45] to study the influence of spatial gluons on the chiral symmetry patterns of the high-spin meson spectrum.

ACKNOWLEDGMENTS

Discussions with G. Burgio, D. Campagnari, M. Quandt and P. Watson are greatly acknowledged. This work was supported by BMBF 06TU7199, by the Europäisches Graduiertenkolleg "Hadronen im Vakuum, Kernen und Sternen," and by the Graduiertenkolleg "Kepler-Kolleg: Particles, Fields and Messengers of the Universe." M. P. acknowledges support by the Austrian Science Fund (FWF) through Grant No. P21970-N16.

[1] C. Feuchter and H. Reinhardt, Phys. Rev. D **70**, 105021 (2004).
[2] D. Schutte, Phys. Rev. D **31**, 810 (1985).
[3] A. P. Szczepaniak and E. S. Swanson, Phys. Rev. D **65**, 025012 (2001).
[4] J. Greensite, H. Matevosyan, Š. Olejník, M. Quandt, H. Reinhardt, and A. P. Szczepaniak, Phys. Rev. D **83**, 114509 (2011).
[5] D. Epple, H. Reinhardt, and W. Schleifenbaum, Phys. Rev. D **75**, 045011 (2007).
[6] G. Burgio, M. Quandt, and H. Reinhardt, Phys. Rev. Lett. **102**, 032002 (2009).
[7] W. Schleifenbaum, M. Leder, and H. Reinhardt, Phys. Rev. D **73**, 125019 (2006).
[8] H. Reinhardt and D. Epple, Phys. Rev. D **76**, 065015 (2007).
[9] M. Pak and H. Reinhardt, Phys. Rev. D **80**, 125022 (2009).
[10] H. Reinhardt, Phys. Rev. Lett. **101**, 061602 (2008).
[11] M. Leder, J. M. Pawlowski, H. Reinhardt, and A. Weber, Phys. Rev. D **83**, 025010 (2011).

[12] G. Burgio, M. Quandt, and H. Reinhardt, Phys. Rev. D **86**, 045029 (2012).
[13] H. Reinhardt, D. Campagnari, and A. Szczepaniak, Phys. Rev. D **84**, 045006 (2011).
[14] J. Heffner, H. Reinhardt, and D. R. Campagnari, Phys. Rev. D **85**, 125029 (2012).
[15] J. Fingberg, U. M. Heller, and F. Karsch, Nucl. Phys. **B392**, 493 (1993).
[16] O. Kaczmarek, F. Karsch, P. Petreczky, and F. Zantow, Phys. Lett. B **543**, 41 (2002).
[17] B. Lucini, M. Teper, and U. Wenger, J. High Energy Phys. 02 (2005) 033.
[18] H. Reinhardt and J. Heffner, Phys. Lett. B **718**, 672 (2012).
[19] H. Reinhardt and J. Heffner, Phys. Rev. D **88**, 045024 (2013).
[20] Y. Nambu and G. Jona-Lasinio, Phys. Rev. **122**, 345 (1961).
[21] Y. Nambu and G. Jona-Lasinio, Phys. Rev. **124**, 246 (1961).
[22] D. Ebert and H. Reinhardt, Nucl. Phys. **B271**, 188 (1986).
[23] J. R. Finger and J. E. Mandula, Nucl. Phys. **B199**, 168 (1982).
[24] A. Le Yaouanc, L. Oliver, O. Pene, and J. Raynal, Phys. Rev. D **29**, 1233 (1984).
[25] S. L. Adler and A. Davis, Nucl. Phys. **B244**, 469 (1984).
[26] P. J. de A. Bicudo and J. E. F. T. Ribeiro, Phys. Rev. D **42**, 1611 (1990).
[27] R. Alkofer and P. Amundsen, Nucl. Phys. **B306**, 305 (1988).
[28] F. J. Llanes-Estrada, S. R. Cotanch, A. P. Szczepaniak, and E. S. Swanson, Phys. Rev. C **70**, 035202 (2004).
[29] C. Fontoura, G. Krein, and V. Vizcarra, Phys. Rev. D **87**, 025206 (2013).
[30] M. Pak and H. Reinhardt, Phys. Lett. B **707**, 566 (2012).
[31] P. Watson and H. Reinhardt, Phys. Rev. D **75**, 045021 (2007).
[32] P. Watson and H. Reinhardt, Phys. Rev. D **77**, 025030 (2008).
[33] P. Watson and H. Reinhardt, Phys. Rev. D **85**, 025014 (2012).
[34] N. Christ and T. Lee, Phys. Rev. D **22**, 939 (1980).
[35] V. Gribov, Nucl. Phys. **B139**, 1 (1978).
[36] D. R. Campagnari and H. Reinhardt, Phys. Rev. D **82**, 105021 (2010).
[37] A. Voigt, E.-M. Ilgenfritz, M. Muller-Preussker, and A. Sternbeck, Phys. Rev. D **78**, 014501 (2008).
[38] Y. Nakagawa, A. Nakamura, T. Saito, and H. Toki, Phys. Rev. D **83**, 114503 (2011).
[39] J. Greensite and S. Olejnik, Phys. Rev. D **67**, 094503 (2003).
[40] D. Zwanziger, Phys. Rev. Lett. **90**, 102001 (2003).
[41] H. Reinhardt, *Quantenmechanik 2* (Oldenbourg-Verlag, München, 2013).
[42] G. Burgio, M. Schrock, H. Reinhardt, and M. Quandt, Phys. Rev. D **86**, 014506 (2012).
[43] D. Epple, H. Reinhardt, W. Schleifenbaum, and A. Szczepaniak, Phys. Rev. D **77**, 085007 (2008).
[44] D. Campagnari and H. Reinhardt (to be published).
[45] M. Pak and L. Y. Glozman, Phys. Rev. D **88**, 076010 (2013).